RC 1100'10 d&J.

RECD 23 SEP 2004
WIPO PCT

PA 1220397

THE UNITED STATES OF AMERICA

TO ALL TO WHOM THESE PRESENTS SHALL COME:

UNITED STATES DEPARTMENT OF COMMERCE

United States Patent and Trademark Office

September 09, 2004

THIS IS TO CERTIFY THAT ANNEXED HERETO IS A TRUE COPY FROM THE RECORDS OF THE UNITED STATES PATENT AND TRADEMARK OFFICE OF THOSE PAPERS OF THE BELOW IDENTIFIED PATENT APPLICATION THAT MET THE REQUIREMENTS TO BE GRANTED A FILING DATE UNDER 35 USC 111.

APPLICATION NUMBER: ***60/510,595***
FILING DATE: ***October 10, 2003***

PRIORITY DOCUMENT
SUBMITTED OR TRANSMITTED IN COMPLIANCE WITH RULE 17.1(a) OR (b)

By Authority of the
COMMISSIONER OF PATENTS AND TRADEMARKS

N. WOODSON
Certifying Officer

15992 U.S.PTO

101003

PTO/SB/16 (6-95)
Approved for use through 04/11/98. OMB 0651-0037
Patent and Trademark Office; U.S. DEPARTMENT OF COMMERCE

PROVISIONAL APPLICATION COVER SHEET

This is a request for filing a PROVISIONAL APPLICATION under 37 CFR 1.53 (b)(2).

Docket Number	103.0009 PSP	Type a plus sign (+) inside this box -->	+

60/510595 U.S. PTO 101003

INVENTOR(s)/APPLICANT(s)			
LAST NAME	FIRST NAME	MIDDLE INITIAL	RESIDENCE (CITY AND EITHER STATE OR FOREIGN COUNTRY)
DAOUD JALALI	AHMED YOUNES	M.	1 Hansel Dr., Apt. V2L, College Station, TX 77840 3 Penarth Place, Cambridge CB3 9LU, U.K.

TITLE OF THE INVENTION (280 characters max)

ZONAL ALLOCATION IN TWO-LAYERS VERTICAL/DEVIATED PRODUCING WELLS USING DISTRIBUTED TEMPERATURE SENSING

CORRESPONDENCE ADDRESS

Patent Counsel, Schlumberger Technology Corporation,
P.O. Box 1590, Rosharon

STATE	Texas	ZIP CODE	77583-1590	COUNTRY	U.S.A.

ENCLOSED APPLICATION PARTS *(check all that apply)*

[X]	Specification	*Number of Pages* 57	[ ]	Small Entity Statement	
[ ]	Drawing(s)	*Number of Sheets* 0	[X]	Other (specify)	Post Card

METHOD OF PAYMENT *(check one)*

[ ]	A check or money order is enclosed to cover the Provisional filing fees	PROVISIONAL FILING FEE AMOUNT ($)	$160.00
[X]	The Commissioner is hereby authorized to charge filing fees and credit Deposit Account Number: 50-2475		

The invention was made by an agency of the United States Government or under a contract with an agency of the United States Government.

[X] No.

[ ] Yes, the name of the U.S. Government agency and the Government contract number are: _____

Respectfully submitted,

SIGNATURE Jaime A. Castano Date 10/10/2003

TYPED or PRINTED NAME Jaime A. Castano REGISTRATION NO. *(if appropriate)* 41,660

[ ] Additional inventors are being named on separately numbered sheets attached hereto

PROVISIONAL APPLICATION FILING ONLY

IN THE UNITED STATES PATENT & TRADEMARK OFFICE

Applicant: Daoud et al. Attorney Docket No: 103.0009 PSP

Serial No: Art Unit:

Filed: Examiner:

For: **Zonal Allocation in Two-Layers Vertical/Deviated Producing Wells Using Distributed Temperature Sensing**

Mail Stop: Provisional Patent Application
Commissioner for Patents
P.O. Box 1450
Alexandria, VA 22313-1450

CERTIFICATE OF MAILING

I hereby certify that this Provisional Patent Application is being deposited with the United States Postal Service as Express Mail No. EV 335 954 142 US in an envelope addressed to: Mail Stop: Provisional Patent Application, Commissioner for Patents, P.O. Box 1450, Alexandria, VA 22313-1450.

Joanne C. Hyland 10/10/03

Date

Joanne C. Hyland
Schlumberger Technology Corporation
14910 Airline Road
Rosharon, Texas 77583-1590

IN THE UNITED STATES PATENT & TRADEMARK OFFICE

United States Provisional Patent Application

For

Zonal Allocation in Two-Layers Vertical/Deviated Producing Wells Using Distributed Temperature Sensing

By

Ahmed Mohamed Daoud and Younes Jalali

CERTIFICATE OF MAILING UNDER 37 C.F.R. 1.8 & 1.10

I hereby certify that this document and its attachments are being sent on the date indicated below to: Mail Stop: Patent Application, Commissioner for Patents, P.O. Box 1450, Alexandria, VA 22313-1450

- ☐ facsimile to number _____.
- ☐ first class mail.
- ☐ Express Mail: Post Office to Addressee No. EV 335 954 142

10/10/03 — Joanne Gaylord

Date

TABLE OF CONTENTS

LIST OF SYMBOLS

$\hat{U}$ = Specific internal energy, BTU/lbm

$\hat{H}$ = Specific enthalpy, BTU/lbm

$\hat{V}$ = Specific volume, ft^3/lbm

α = Thermal diffusivity of earth, ft^2/hr

μ = Viscosity, cp

ϕ = Constant for friction factor given by Eq. 2.36

θ = Angle of inclination of the well with horizontal, degrees

ρ = Density, lbm/ft^3

μ_1 = Viscosity of the fluid flowing from the lower zone, cp

ρ_1 = Density of the fluid produced from lower producing zone, lbm/ft^3

μ_2 = Viscosity of the fluid flowing from the upper zone, cp

ϕ_D = Dimensionless number, given by Eq. 2.41

ρ_e = Earth density, lbm/ft^3

γ_g = Gas specific gravity (air = 1)

μ_{JT} = Joule Thomson coefficient, F/psi

ρ_o = Oil density, lbm/ft^3

γ_o = Oil specific gravity

μ_{o1} = Viscosity of oil produced from the lower producing zone, cp

μ_{o2} = Viscosity of oil produced from the upper producing zone, cp

ρ_w = Water density, lbm/ft^3

γ_w = Water specific gravity,

μ_{w1} = Viscosity of water produced from the lower producing zone, cp

μ_{w2} = Viscosity of water produced from the upper producing zone, cp

A_D = Dimensionless number given by Eq. 2.40

B = Formation volume factor, bbl/stb

C_e = Specific heat of earth, BTU/lbm-F

C_p = Specific heat of liquid, BTU/lbm-F

$C_{p(i)}$ = Specific heat of liquid inside the producing zone, BTU/lbm-F

C_{p1} = Specific heat of liquid produced from the lower zone, BTU/lbm-F

C_{p2} = Specific heat of liquid produced from the upper zone, BTU/lbm-F

$C_{p5'}$ = Specific heat of liquid at node 5`, BTU/lbm-F

C_{pM} = Specific heat of liquid after the mixing, BTU/lbm-F

C_{po} = Specific heat of oil, BTU/lbm-F

C_{pw} = Specific heat of water, BTU/lbm-F

f = Friction factor

g = Acceleration of gravity, 32.2 ft/sec^2

g_c = Conversion factor, 32.2 ft-lbm/sec^2-lbf

GLR = Gas liquid ratio, scf/stb

G_T = Geothermal gradient, F/ft

h = Formation thickness, ft

i = Index for number of temperature measurements in the producing zones

I_0 = Modified Bessel function I of order 0

I_1 = Modified Bessel function I of order 1

J = Conversion factor, 778 ft-lbf/BTU

K = Permeability, md

K.E. = Kinetic Energy

K_0 = Modified Bessel function K of order 0

K_1 = Modified Bessel function K of order 1

K_{an} = Thermal conductivity of material in annulus, BTU/D-ft-F

K_{anw} = Thermal conductivity of water in annulus, BTU/D-ft-F

K_{cem} = Thermal conductivity of cement, BTU/D-ft-F

K_e = Thermal conductivity of earth, BTU/D-ft-F

L = Total length of the well, ft

m = Vector for input parameters for the forward model

n = Total number of temperature measurements in the producing zone

O = Objective function

P = Pressure, psi

P.E. = Potential Energy

P_e = Reservoir pressure. psi

P_{wf} = Flowing well pressure, psi

q = Flow rate

Q = Heat transfer between fluid and surrounding area, BTU/lbm

q_1 = Flow rate from the lower producing zone

q_2 = Flow rate from the upper producing zone

q_o = Oil flow rate, STB/D

q_{o1} = Oil flow rate from the lower zone, STB/D

q_{o2} = Oil flow rate from the upper zone, STB/D

q_{oT} = Total oil flow rate from the two zones, STB/D

q_w = Water flow rate, STB/D

q_{w1} = Water flow rate from the lower zone, STB/D

q_{w2} = Water flow rate from the upper zone, STB/D

q_{wT} = Total water flow rate from the two zones, STB/D

r = Radius, in

r_{ci} = Inside casing radius, in

r_{co} = Outside casing radius, in

r_D = Dimensionless radius

R_e = Reynolds number, dimensionless

r_e = Drainage radius, ft

r_{eD} = Dimensionless drainage radius

r_{ti} = Inside tubing radius, in

r_{to} = Outside tubing radius, in

r_{wb} = Well bore radius, in

s = Dummy variable in the Laplace domain

t = Time, hr

T = Temperature, F

T_5 = Temperature at node 5, F

$T_{5'}$ = Temperature at node 5`, F

T_6 = Temperature at node 6, F

t_D = Dimensionless time

T_e = Earth temperature, F

T_{eD} = Earth dimensionless temperature

T_{ei} = Earth temperature at any depth and far away from the well, F

T_{eibh} = Earth temperature at the bottom hole of the well, F

T_f = Fluid temperature at any depth, F

$T_{f(i)}$ = Flowing temperature in the well in front of the upper producing zone, F

T_{fbh} = Fluid temperature at the bottom hole of the well, F

$T_{fbh(i)}$ = Flowing temperature in the well in front of the lower producing zone, F

T_{fbh1} = Temperature in the well bore at the bottom of the lower producing zone, F

T_{fbh2} = Temperature in the well bore at the top of the lower producing zone, F

T_{fD} = Dimensionless fluid temperature

T_{fdbh} = Dimensionless temperature in the well bore at the fluid entry for each well section, F

T_h = Temperature at the cement/earth interface, F

T_i^{cal} = Calculated temperature, F

T_i^{obs} = observed or measured temperature, F

U = Overall heat transfer coefficient, BTU/D-ft^2-F

v = Local fluid velocity, ft/sec

w_t = Total mass flow rate, lbm/sec

z = Height from the bottom of the hole, ft

z_D = Dimensionless height

z_{dbh} = Dimensionless Depth at the fluid entry for each well section

SUMMARY

Recently the fiber optic technology has been introduced to the petroleum industry and one of its main advantages is to get continuous measurements of temperatures in space and time inside the wells. There are different applications of temperature measurements; one of its main applications inside the producing wells is zonal rates allocation from different producing zones. Due to the weak relationship between the temperature and the zonal rates, so the main objective of this study is to develop a rigorous mathematical forward model of temperature as function of zonal rates and some other fluid and thermal properties starting from the basic balance equations. Then, use this forward model as a tool in inversion to invert the measured temperature to allocate the rates from the different producing zones. A simple forward model suitable for handy calculations has been obtained for two-phase (oil-water) two zones producing wells. The accuracy of the inversion for the zonal allocation from temperature measurements has been examined using synthetic examples for single and two-phase oil-water flow under different conditions. In addition the forward model has been tested on field data taken from a producing well where a fiber optic distributed temperature sensors (DTS) has been installed to test the forward modeling and to validate the findings from the synthetic examples. The forward modeling shows a good agreement with the field data of maximum difference less than 1 F and the results of the inversion from the synthetic and field examples reveal the important of imposing the total rate as constraint during the inversion especially for low temperature contrast between the producing zones.

Chapter 1

INTRODUCTION

[1.1] Objectives

Since the introduction of the permanent down hole fiber-optic sensors to the oil and gas industry in early 1990 and many works have been done to try to implement this technology and study its application. Since the last two years, Schlumberger has been deeply involved in the application of this technology[1] and they developed SENSA distributed temperature sensing (DTS) where the temperature measurements inside production and injection wells can be done continuously in space and time, temperature can be obtained every 7 seconds and collected every 3.3 ft[1]. These continuous measurements of temperature have many applications in the oil and gas industry, one of these applications is to know when and from where the production occurs in a producing wells and the most important is how much flow is taken place from multi-laterals producing wells. Accordingly, the objective of this work is to study the availability of using the DTS measurements in quantifying the zonal rates from multi-zones producing wells and test how accurate is these quantifications.

[1.2] Working Steps

To achieve the above objectives, the following steps have been taken:

1- Developing a simple analytical forward modeling that describes the temperature profile in a single phase oil/water, single layer producing well that capture most of the physics of the problem

2- Make a comparison with the other known models and with the numerical solution available in Eclipse 300 under the thermal option.

3- Reformulate the forward model to be applied for a single liquid phase two layers production well and extend the modeling to two-phase oil and water production.

4- Show the concept of the inverse modeling to invert the temperature measurements to estimate the rates from the different producing zones by the aid of some synthetic examples. The objective of these synthetic examples is to:

i- Study the availability to invert the temperature for the zonal rates under different conditions.

ii- Do uncertainty analysis to see the effect of the uncertainty of the model parameters on the accuracy of rate allocation from different zones.

5- Test the application of the forward and the inverse modeling on a field case using DTS measurements in one of highly deviated production well

So the organization of the report will be as follows, the second chapter will concern with the first two points, the third chapter will handle the third point, the fourth chapter will cover the fourth point, the fifth chapter will be mainly for the field case application, and finally, the sixth chapter will be devoted for conclusions and recommendation for future works, mainly the extension of the forward modeling to handle multi-phase production.

Chapter 2

TEMPERATURE FORWARD MODELING IN SINGLE LAYER PRODUCTION WELLS & MODEL SELECTION

The objective of this chapter is to show the mathematical formulation of the temperature modeling in vertical or deviated producing well from a single layer-single phase liquid production, propose different models by either including or neglecting some model parameters, and finally compare all the proposed models and the well known models from the literature with the numerical modeling obtained from Eclipse 300 under the thermal option in order to select the best model for a single layer production and then use this model for extending the modeling to more than one layer production.

[2.1] Mathematical Formulation of the Temperature Modeling

Fig. 2.1 shows the thermal nodal analysis used to develop a mathematical temperature model by determining the temperature at each node using mass, momentum and energy balance equations.

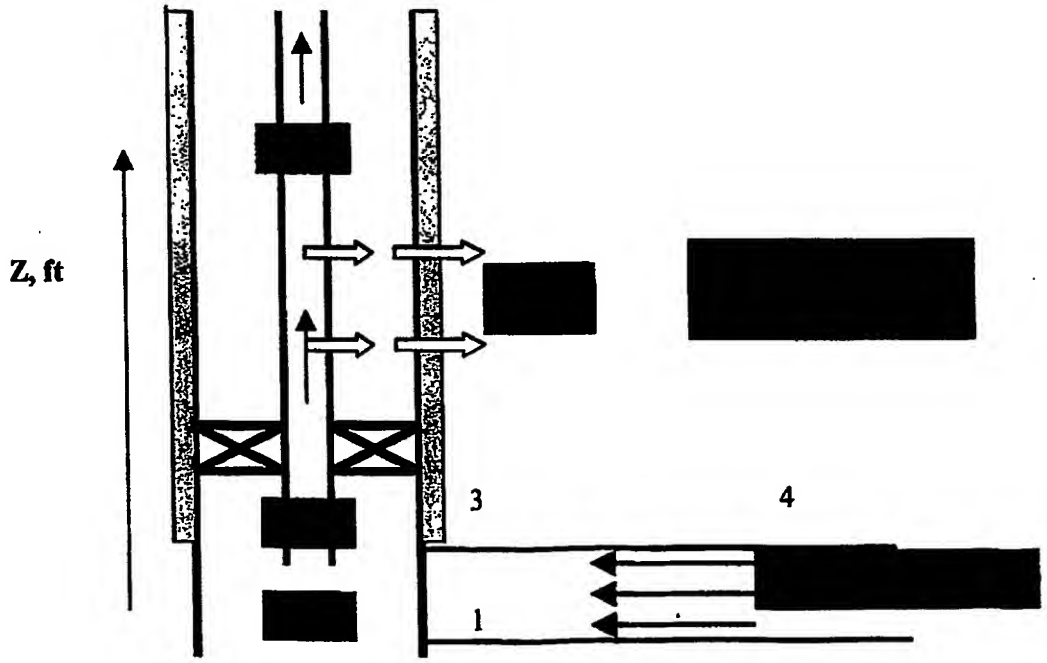

Fig 2.1: Schematic diagram showing the nodal temperature analysis in tubing and in formation.

Table 2.1 shows the temperature nomenclature at each node presented in Fig. 2.1.

Table 2.1: Temperature Nomenclature at each node

Node	Nomenclature
1	Bottom hole formation temperature calculated from the earth geothermal gradient, T_{eibh}
2	Bottom hole flowing fluid temperature, T_{fbh1}
2`	Flowing fluid temperature at the top of the producing zone, T_{fbh2}
3	Formation temperature at the well/earth interface in the non-producing zone
4	Formation temperature calculating from the earth geothermal gradient in the non producing zone, T_{ei}
5	Flowing temperature, T_f, and it can be at any depth Z from the producing zone

Depending upon the transport phenomena, whether mass, momentum, or energy, between each node, the balance equation is used. The following diagram, Fig. 2.2 shows the type of balance equation and the assumptions used in each equation. These assumptions are taken based on the previous works of many authors and also to try to keep the equation easy to implement and at the same time does not violate the physics of the problem.

The material balance equation in general form is written as follows:

Mass Balance Equation:

Rate of increase of mass = rate of mass in – rate of mass out .....*(2.0)*

Momentum Balance Equation:

Rate of increase of momentum = rate of momentum in – rate of momentum out + external force on the fluid .....*(2.00)*

Energy Balance Equation:

Rate of change of (internal energy + K.E.+P.E. due to convection)+(net rate of heat addition by conduction)-(net rate of work done by the system on the surrounding) = (Rate of accumulation of internal energy + K.E + P.E) .....*(2.000)*

For the reader convenience, I highly recommend to return to see the general mathematical equation for the above three balance equations in Bird et al book[2] (Table 11.4-1, page 341)

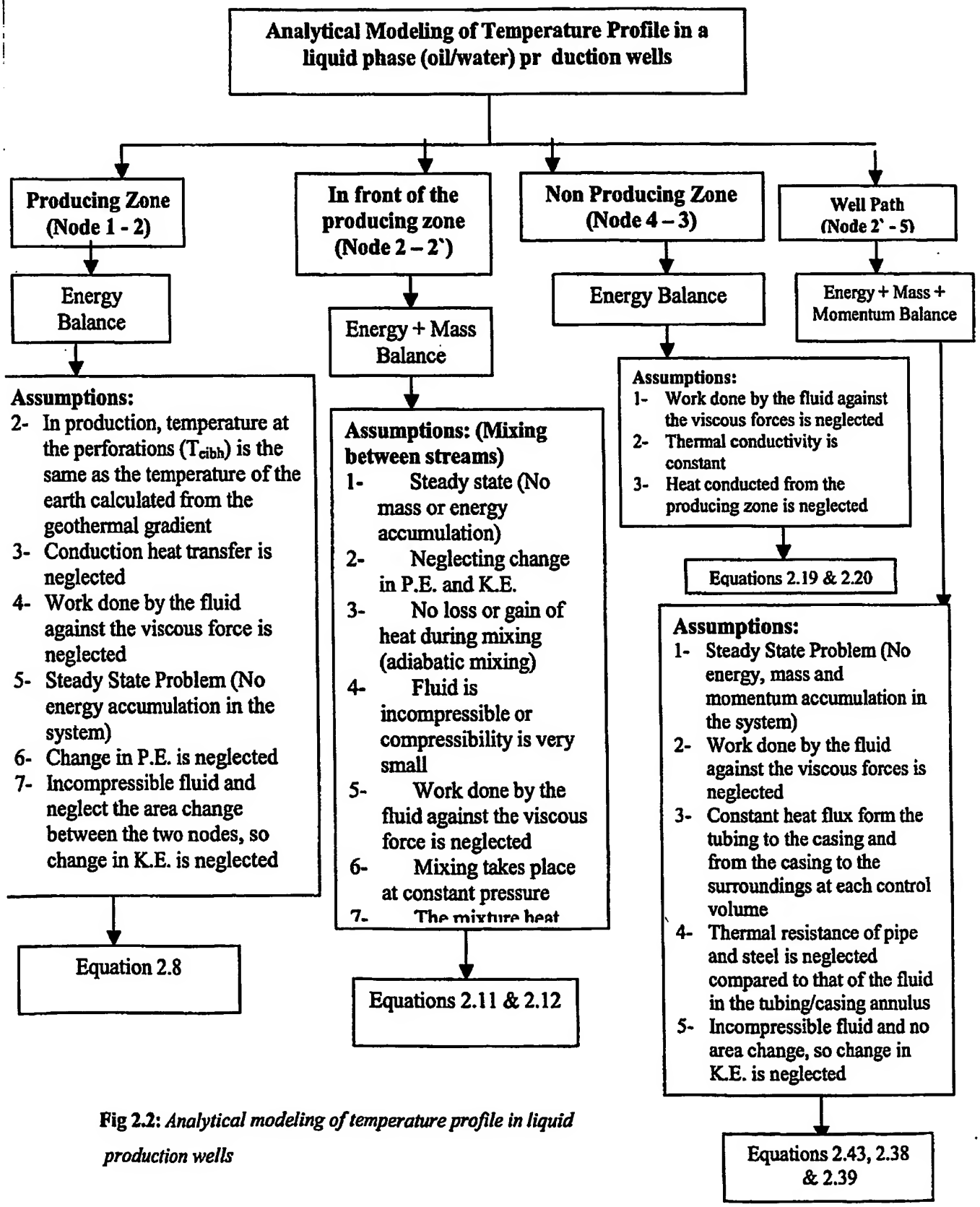

Fig 2.2: *Analytical modeling of temperature profile in liquid production wells*

[2.1.1] Producing zone (node 1 and 2)

The general energy balance equation written in term of enthalpy instead of internal as presented in Bird et al[2] is as following:

Rate of change of (enthalpy+ K.E.+P.E. due to convection)+(net rate of heat addition by conduction)-(net rate of work done by the system on the surrounding) = (Rate of accumulation of enthalpy + K.E + P.E) .....(2.1)

According to the assumptions mentioned in Fig. 2.2 for node (1-2), the general energy balance equation, Eq. 2.1 will be:

$$d\hat{H} = 0.0 \qquad \text{.....(2.2)}$$

From the basic thermodynamic principles, $d\hat{H}$ can be obtained from the following equation[3],

$$d\hat{H} = C_p dT - \mu_{JT} C_p dP \qquad \text{.....(2.3)}$$

Where, μ_{JT} is the Joule Thomson coefficient and can be obtained from the following equation[3,4]:

$$\mu_{JT} = \left[\frac{\partial T}{\partial p}\right]_{\hat{H}} = \frac{1}{C_p}\left[T\left(\frac{\partial \hat{V}}{\partial T}\right)_p - \hat{V}\right] \qquad \text{.....(2.4)}$$

For incompressible or slightly compressible fluid, $\rho = cons\tan t$, $\hat{V} = cons\tan t$

$$\therefore \left[\frac{\partial \hat{V}}{\partial T}\right]_{\hat{p}} = 0.0 \qquad \text{.....(2.5)}$$

From Eqs. 2.5, 2.4, and 2.2, Eq. 2.3 will be

$$d\hat{H} = C_p dT + \hat{V} dP = 0.0 \qquad \text{.....(2.6)}$$

$$\therefore C_p dT = -\frac{dP}{\rho} \qquad \text{.....(2.7)}$$

Solving Eq. 2.7 leads to Eq 2.8, which is written in the field unit as follows:

$$T_{fbh1} = T_{eibh} + \frac{144 \cdot (P_e - P_{wf})}{\rho_f \cdot C_p \cdot J} \qquad \text{.....(2.8)}$$

Eq. 2.8 indicates that only the effect of Joule Thompson coefficient is dominant in calculating the temperature at node 2 by knowing the temperature at node 1 due to the

flow through the perforations. The pressure drop can be calculated using Darcy's equation by knowing reservoir rock and fluid properties and assuming a steady state flow[5]:

$$(P_e - P_{wf}) = \frac{141.2\, q\, \mu\, B}{K\, h} \ln\left(\frac{r_e}{r_{wb}}\right) \qquad \text{.....(2.9)}$$

[2.1.2] In front of the Producing zone (node 2 – 2`)

In this part, to obtain an expression for the temperature, we need to divide the producing zone into equal intervals, each interval producing equal rate. The number of divisions depends upon the number of temperature measurements in the producing zone. By applying a macroscopic mass and energy balance[2] due to the mixing of two streams, we can get the temperature at the any interval inside the producing zone using the following derived equation:

$$T_{fbh(i)} = \frac{q_{i-1}\, C_{p(i-1)} T_{fbh(i-1)} + q_i\, C_{p(i)}\, T_{ei}}{q_{i-1}\, C_{p(i-1)} + q_i\, C_{p(i)}} \qquad \text{.....(2.10)}$$

Where, i = 2, 3,....., n (n is the number of temperature measurements inside the producing zone), taking into consideration that T_{fbh1} is calculated from Eq. 2.8 and 2.9 before. Also, T_{ei} should be corrected due to the pressure drop across the perforation using the same Eqs. 2.8 and 2.9 but using T_{ei} instead of T_{eibh}

As the fluids produced from each interval inside the producing zone have equal rate and equal specific heat capacity, C_p, so Eq. 2.10 can be written in the following form:

$$T_{fbh(i)} = \frac{(i-1)\, T_{fbh(i-1)} + T_{ei}}{i} \qquad \text{.....(2.11)}$$

Accordingly, temperature at node 2` will be:

$$T_{fbh2} = T_{fbh(n)} \qquad \text{.....(2.12)}$$

It should be noted that Eq. 2.11 is rate independent as it depends upon assuming that at each interval inside the producing zone, the producing rates are equal and the sum of those individual rates is the total producing rate from this producing zone, accordingly we should impose a condition such that at no production or physically at neglected production, Eqs. 2.10 and 2.11 does not hold and in this case the temperatures inside the producing zone should be equal to the geothermal temperature.

For the synthetic cases, and to simplify the calculation, we can assume that only one temperature measurement inside the producing zone (one single entry) and in this case temperature at node 2` is the same as at node 2.

[2.1.3] Non Producing zone (node 4 -3)

As the fluid produced, heat is transferred by convection inside the well bore and some of this heat is lost by conduction to the non-producing formation. Thus, inside the non-producing zone, the transport phenomenon is only the heat energy due to heat loss from the well bore to the non-producing zone. So the only balance equation required is the energy balance equation.

By applying the general energy balance equation given in Eq. 2.1 between node 3 and 4 and according to the assumptions mentioned in Fig. 2.2 for node (4-3), the equation becomes:

$$\frac{\partial^2 T_e}{\partial r^2}+\frac{1}{r}\frac{\partial T_e}{\partial r}=\frac{c_e \rho_e}{K_e}\frac{\partial T_e}{\partial t} \qquad \text{.....(2.13)}$$

It should be mentioned that Eq. 2.13 is in 1D radial with the most common assumption that the earth density is unvaried with space and also with constant earth thermal conductivity.

Eq.2.13 can be converted to the dimensionless form by using the following dimensionless variables according to Hasan and Kabir[6]:

$$T_{eD}=-\frac{2\pi K_e}{w_t(\frac{dQ}{dz})}(T_h-T_{ei}) \qquad \text{.....(2.14)}$$

Where T_h is the temperature at node 3

$$r_D=\frac{r}{r_{wb}} \qquad \text{.....(2.15)}$$

$$t_D=\frac{K_e}{\rho_e c_e r_{wb}^2}t=\frac{\alpha}{r_{wb}^2}t \qquad \text{.....(2.16)}$$

The radial partial differential equation of temperature distribution in earth in dimensionless form will be:

$$\frac{\partial^2 T_{eD}}{\partial r_D^2}+\frac{1}{r_D}\frac{\partial T_{eD}}{\partial r_D}=\frac{\partial T_{eD}}{\partial t_D} \qquad \text{.....(2.17)}$$

Eq.2.17 can be solved using the following initial and boundary conditions:

Initial Condition: $\lim_{t_D\to 0} T_{eD}=0$, Temperature is constant (equal T_{ei}, which is the earth temperature at any given depth and at infinite distance away from the well, temperature at node 4).

Boundary Conditions:

Outer Boundary Condition: $\lim_{r_D\to r_{eD}} \frac{\partial T_{eD}}{\partial r_D}=0$ (No change in temperature at infinite r_D)

Inner Boundary Condition: $\left.\frac{\partial T_{eD}}{\partial r_D}\right|_{r_{D=1}}=-1$ (rate of flow of heat from the well bore to the surrounding earth across an element dz is constant).

Eq. 2.17 is converted to the Laplace domain and is solved using **Mathematica software.** The solution of T_{eD} in the Laplace domain ($T_{eD}(s)$) is in the following form:

$$\frac{I_1(\sqrt{s}\ r_{eD})\cdot K_0(\sqrt{s}\cdot r_D)+I_0(\sqrt{s}\cdot r_D)\cdot K_1(\sqrt{s}\cdot r_{eD})}{s^{3/2}\left[I_1(\sqrt{s}\cdot r_{eD})\cdot K_1(\sqrt{s})-I_1(\sqrt{s})\cdot K_1(\sqrt{s}\cdot r_{eD})\right]} \qquad \text{.....(2.18)}$$

Where, s is a dummy variable for the Laplace domain, and I_0, I_1, K_0, K_1 are the modified Bessel functions. Eq. 2.18 is the cylindrical source solution of Eq. 2.17 which is difficult to be inverted to the time domain analytically, so I used the Gaver functional, Wynn-Rho algorithm that is coded in **Mathematica** to get the inversion numerically by setting r_{eD} to a very high value (e.g. 1000) and r_D to 1 as we are interested to get the T_{eD} at the well/earth interface. Fig. 2.3 shows the T_{ed} versus t_D at the well/earth interface.

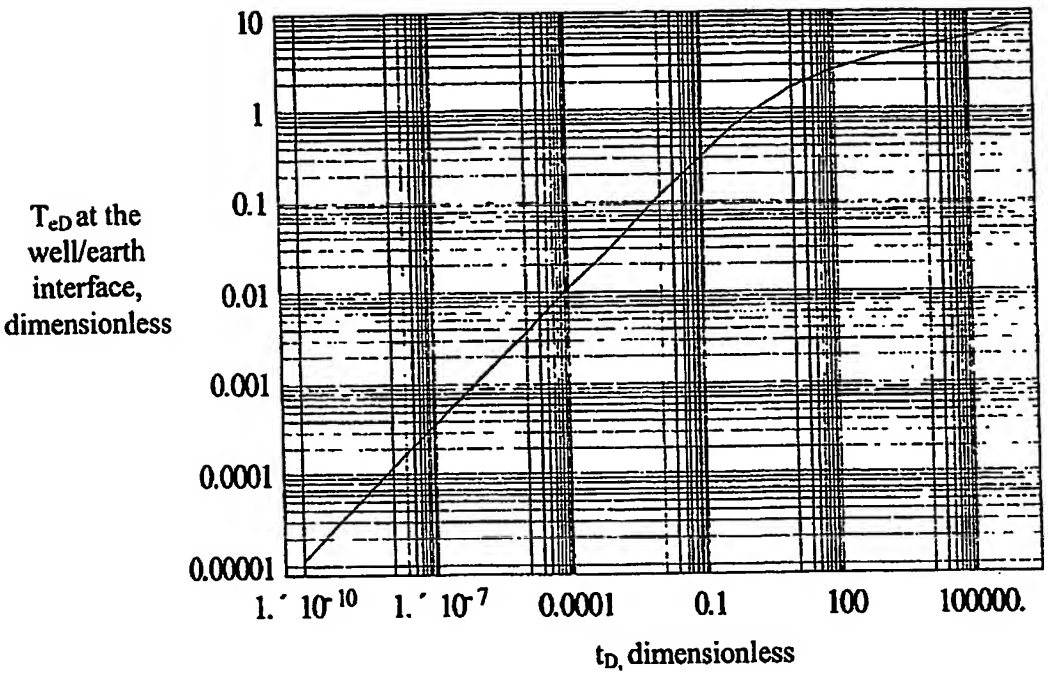

***Fig. 2.3:** Log-Log plot of T_{ed} versus t_D at the well/earth interface*

Hasan & Kabir[6] have done an approximation to the solution of Eq. 2.17 at the well/earth interface using the same initial and boundary condition and got the following equation:

$$T_{eD}\big|_{r_D=1} = 1.1281\sqrt{t_D}\left[1-0.3\sqrt{t_D}\right] \qquad \text{if } t_D \le 1.5 \qquad \text{.....(2.19)}$$

$$T_{eD}\big|_{r_D=1} = \left[0.4063+0.5\ln(t_D)\right]\cdot\left[1+\frac{0.6}{t_D}\right] \qquad \text{if } t_D > 1.5 \qquad \text{.....(2.20)}$$

A comparison between the solution using the numerical laplace inversion and that obtained from Hasan & Kabir[6] solution is given in Fig. 2.4, the comparison shows that most of the points range from 10^{-10} days to 10000 days lies on a 45° line, so for simplicity, Hasan and Kabir[6] solution, Eqs. 2.19 and 2.20 is used to get the temperature at node 3 by knowing the temperature at node 4 obtained from the geothermal gradient.

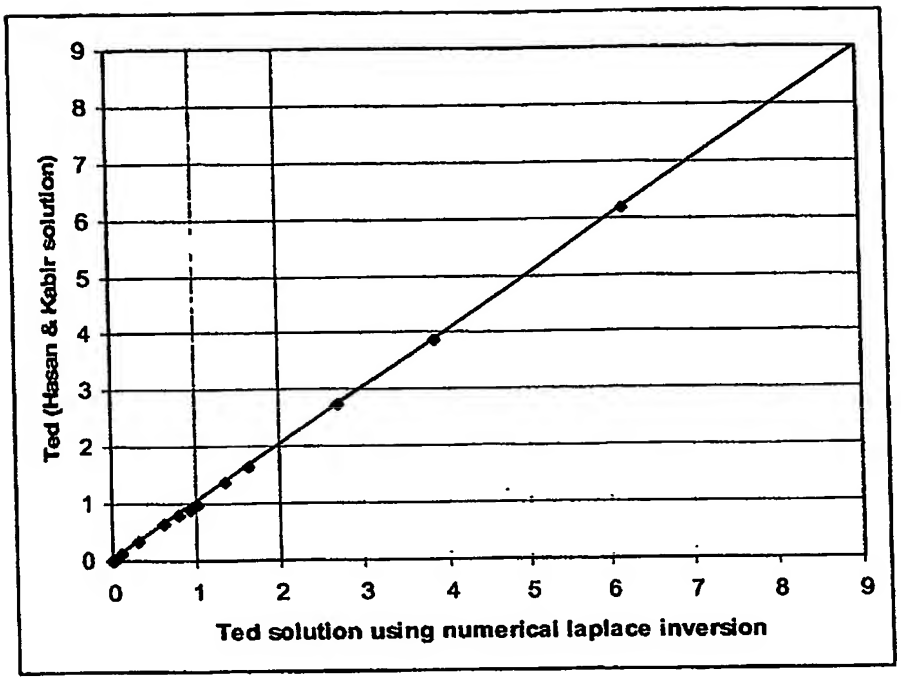

Fig. 2.4: Comparison between the numerical laplace inversion solution and Hasan & Kabir solution for Ted at the well/earth interface

[2.1.4] Well Path (node 2`- 5)

As the fluid proceeds from node 2` to 5, heat energy is transported by convection and also mass and momentum are transported due to the fluid flow. So, energy, mass, and momentum balance equations are applied between node 2` and 5.

The general energy and mass balance equation after applying the assumptions mentioned in Fig. 2.2 will be:

$$\frac{d\hat{H}}{dz} = -\frac{\partial Q}{\partial z} - v\frac{\partial v}{\partial z} - g\,\mathrm{Sin}\theta \qquad \text{.....(2.21)}$$

For radial heat transfer from the well bore fluid to the well (cement) /earth interface,

$$\frac{dQ}{dz} = \frac{2\pi\, r_{ti}\, U}{w_t}(T_f - T_h) \qquad \text{.....(2.22)}$$

Where, T_h is the temperature at node 3 and w_t is the total mass flow rate, which is calculated as follows[3]:

$$w_t = \frac{q_g \gamma_g}{1.1309 \times 10^6} + \frac{q_w \gamma_w + q_o \gamma_o}{246.6} \qquad \text{.....(2.22a)}$$

The radial heat transfer from the well (cement)/earth interface to the surrounding can be obtained from Eq. 2.14 which is the definition of the dimensionless earth temperature,

$$\frac{dQ}{dz} = \frac{2\pi \, r_{ti} \, U}{w_t T_{eD}} (T_h - T_{ei}) \qquad \text{.....(2.23)}$$

From Eq. 2.22 and 2.23,

$$\frac{dQ}{dz} = \frac{2\pi}{w_t} \left[\frac{r_{ti} U K_e}{K_e + T_{eD} r_{ti} U} \right] (T_f - T_{ei}) \qquad \text{.....(2.24)}$$

From the basic thermodynamic principles or from Eq. 2.3, the specific enthalpy can be taken from the following formula:

$$\frac{d\hat{H}}{dz} = -\mu_{JT} c_p \frac{dp}{dz} + c_p \frac{dT_f}{dz} \qquad \text{.....(2.25)}$$

By substituting Eq.2.25 and Eq. 2.24 in Eq. 2.21, the final energy balance equation for the fluid in the producing well will be:

$$c_p \frac{dT_f}{dz} = -\frac{2\pi}{w_t} \left[\frac{r_{ti} U K_e}{K_e + T_{eD} r_{ti} U} \right] (T_f - T_{ei}) - g \, Sin\theta + \mu_{JT} C_p \frac{dp}{dz} - v \frac{dv}{dz} \qquad \text{.....(2.26)}$$

Where, U is the overall heat transfer coefficient and can be calculated from Eq. 2.27 as shown in (Bird et al)[2] under the following conditions according to Sagar et al[3]:

a- Thermal resistance of pipe and steel are negligible compared to the thermal resistance of the fluid in the tubing/casing annulus,

b- Radiation and convection coefficients are negligible and can be ignored

$$U = \left[r_{ti} \frac{\ln\left(\frac{r_{ci}}{r_{to}}\right)}{K_{an}} + r_{ti} \frac{\ln\left(\frac{r_{wb}}{r_{co}}\right)}{K_{cem}} \right]^{-1} \qquad \text{.....(2.27)}$$

Eq. 2.26 is considered as a general equation for the temperature distribution inside the well bore between node 2` and 5 after combining both mass and energy balance equation and according to the assumptions mentioned in fig. 2.2. Eq. 2.26 has been given by different authors[3,7] and can be applied for both single and multi-phase flow.

By applying the momentum and mass balance equation according to the assumptions mentioned in Fig. 2.2, the term $(\frac{dp}{dz})$ can be obtained as follows:

$$\frac{dp}{dz} = -\rho v \frac{dv}{dz} - \rho g \sin\theta - \left.\frac{dp}{dz}\right|_{friction} \qquad \text{.....(2.28)}$$

Substituting Eq. 2.28 in Eq. 2.26,

$$c_p \frac{dT_f}{dz} = -\frac{2\pi}{w_t}\left[\frac{r_{ti} U K_e}{K_e + T_{eD} r_{ti} U}\right](T_f - T_{ei}) - g\,Sin\theta + \mu_{JT} C_p\left(-\rho v \frac{dv}{dz} - \rho g \sin\theta - \left.\frac{dp}{dz}\right|_{friction}\right) - v\frac{dv}{dz}$$

.....(2.29)

The analytical solution to Eq. 2.29 depends upon the joule Thomson coefficient, which is difficult to be obtained for a multi-phase flow. So, to make the problem easy, we have to divide the solution to a single phase liquid (oil or water production), two phase liquid (oil + water production), single-phase gas, and multi phase (oil + water + gas). This chapter is mainly concern to give the analytical solution for single-phase liquid production and the other chapters will give the analytical solution for the two-phase liquid production (oil + water).

For the single phase liquid, I can consider black oil production below the bubble point pressure especially because I am considering only on the analysis of DTS very close to the producing intervals in which the gas hold up is usually very small compared to that on the surface, so that the assumption of constant density and that the pressure is below the bubble point pressure is applicable at a very small interval close to the producing zone for a black oil production. From Eq. 2.4 for $\hat{V} = cons\tan t$, the joule Thomson coefficient becomes:

$$\mu_{JT} = \frac{-1}{\rho C_p} \qquad \text{.....(2.30)}$$

By substituting Eq. 2.30 into Eq. 2.29, and write the equation in field units,

$$\frac{dT_f}{dz} = -\frac{2\pi}{w_t C_p}\left[\frac{r_{ti} U K_e}{K_e + T_{eD}\frac{r_{ti}}{12} U}\right]\cdot\left[\frac{1}{12\times 86400}\right](T_f - T_{ei}) + \frac{144}{J\rho C_p}\left.\frac{dp}{dz}\right|_{friction} \qquad \text{....(2.31)}$$

The pressure loss due to friction can be obtained from the equations mentioned in Beggs and Brill[8] or the technical description of Eclipse 300[9] as follows:

$$\left.\frac{dp}{dz}\right|_{friction} = \frac{2.956\times10^{-12}\, f\, \rho\, q^2}{D_{ti}^5} \qquad \text{.....(2.32)}$$

Where the friction loss coefficient, f, can be obtained as follows:

$$\text{If } R_e \le 2000,\ f = \frac{16}{R_e}\ ,\ \text{if } R_e > 2000\ \ \frac{1}{\sqrt{f}} = -3.6\log\left[\frac{6.9}{R_e} + \left(\frac{e}{3.7 D_{ti}}\right)^{10/9}\right] \qquad \text{.....(2.33)}$$

Where R_e is the Reynolds number and can be obtained as follows:

$$R_e = \frac{0.1231\,\rho\, q}{D_{ti}\,\mu} \qquad \text{.....(2.34)}$$

By substitute Eqs. 2.32, 2.33, and 2.34 into Eq. 2.31, Eq. 2.31 will be:

$$\frac{dT_f}{dz} = -\frac{2\pi}{w_t C_p}\left[\frac{r_{ti} U K_e}{K_e + T_{eD}\frac{r_{ti}}{12}U}\right]\cdot\left[\frac{1}{12\times86400}\right](T_f - T_{ei}) + \phi \qquad \text{.....(2.35)}$$

$$\text{Where, } \phi = \frac{144}{J}\cdot\frac{2.956\times10^{-12}\, f\, q^2}{D_{ti}^5\, C_p} \qquad \text{.....(2.36)}$$

T_{ei} is calculated by knowing the earth temperature at the bottom hole (T_{eibh}), which is a fixed quantity, and the earth temperature gradient using the following equation:

$$T_{ei} = T_{eibh} - G_T\, z \sin\theta \qquad \text{.....(2.37)}$$

Eq. 2.35 can be converted to a dimensionless form using the following dimensionless parameters:

$$T_{fD} = \frac{T_f}{T_{fbh}} \qquad \text{.....(2.38)}$$

$$z_D = \frac{z}{L} \qquad \text{.....(2.39)}$$

$$A_D = \frac{-2\pi L}{w_t c_p}\left[\frac{r_{ti} U K_e}{K_e + T_{eD}\frac{r_{ti}}{12}U}\right]\cdot\left[\frac{1}{12\times86400}\right] \qquad \text{.....(2.40)}$$

$$\phi_D = \frac{\phi\ L}{T_{fbh}} \qquad \text{.....(2.41)}$$

By substituting Eq. 2.37 and the dimensionless forms, Eqs. 2.38 to 2.41, Eq. 2.35 will be:

$$\frac{dT_{fD}}{dz_D} = A_D\,(T_{fD} - \frac{T_{eibh}}{T_{fbh}} + \frac{G_T\,\mathrm{Sin}\theta\,z_D\,L}{T_{fbh}}) + \phi_D \qquad \text{.....(2.42)}$$

The boundary condition used to solve the above ordinary differential equation is $T_{fD}(z_D = 0) = 1$ This means that the temperature at the bottom hole is equal to T_{fbh}. This boundary condition is suitable for dealing with a production from a single layer. Another boundary condition should be used if dealing with the solution of Eq. 2.42 in multi layers producing wells, as we will see in the next chapter. It should be noted here that the origin of the z scale is at the bottom hole as shown in Fig.2.1. The solution of Eq. 2.42 is done using **Mathematica** to get the profile of the dimensionless fluid temperature inside the well in front of the non producing zones as function of the dimensionless depth and the solution is as follows:

$$T_{fD} = \frac{-G_T\,\mathrm{Sin}\theta\ \mathrm{L} - \mathrm{A_D}\,\mathrm{G_T}\,\mathrm{Sin}\theta\ z_D\,\mathrm{L} + \mathrm{A_D}\,T_{eibh} - T_{fbh}\phi_D + \exp(A_D\,z_D)\cdot[G_T\,\mathrm{Sin}\theta\ \mathrm{L} + \mathrm{A_D}(T_{fbh} - T_{eibh}) + T_{fbh}\phi_D]}{A_D\,T_{fbh}}$$

.....(2.43)

Eqs. 2.38 and 2.39 are used to convert the profile from the dimensionless domain to the real domain by knowing the fixed fluid temperature at the bottom hole of the well, T_{fbh}, and the depth of the well, L.

[2.2] Model Selection

The major objective of this part is to compare the model proposed from the first part of this chapter with the existed work in the literature and also with the numerical solution obtained from Eclipse 300 under the thermal option to test the accuracy of the mathematical model proposed. Also, as we can see that the high uncertainness in the proposed model is during modeling the temperature in front of the producing zone (correcting the geothermal temperature due to the Joule Thomson effect because of the pressure drop across the perforation). As in modeling the temperature in this part, we need reservoir information about the flow regime, and some reservoir properties like permeability, drainage radius and the producing thickness, where there is a huge

uncertainty in obtaining those parameters. So, the second objective of this part is to neglect the correction of the geothermal temperature in front of the producing zone due to the pressure drop in other words, neglect the joule Thomson effect in front of the producing zone and compare the results with the numerical and see how much the error will be.

The models used for the comparison with the numerical solution using Eclipse 300 under the thermal option are as follows:

1- Ramey[10] solution for the liquid phase production,

2- Sagar model[3], and

3- The proposed model given by Eq. 2.43, the proposed model is named as "model 3" during the comparison.

As also the second objective is to study the effect of including the Joule Thomson coefficient in front of the producing zone in the temperature modeling, so additional models have been included in the comparison, which are mainly obtained from Eq. 2.43. These models are:

4- The proposed model, which is "model 3" by neglecting the Joule Thomson coefficient in front of the producing zone, this model is named "Model 4",

5- Model obtained from Eq. 2.43 by neglecting the friction loss ($\phi_D = 0$) and neglecting the Joule Thomson coefficient in front of the producing zone, this model named as "model 2",

6- Model obtained from Eq. 2.43 by neglecting the friction loss ($\phi_D = 0$) and including the Joule Thomson coefficient in front of the producing zone, this model is named "model 1"

In addition to the above six models, two other models have been obtained from Ramey and Sagar model by applying the Joule Thomson coefficient on those models in front of the producing zones, these models are named as follows:

7- "Modified Ramey model"

8- "Modified Sagar model"

Table 2.2 shows the well and the reservoir fluid and rock data used by the above eight different models and the numerical model obtained from Eclipse 300 under the thermal option to do the comparison and select the best model.

Table2.2: Input *Data for the numerical (Eclipse 300) and the forward models:*

Well Data	Value	Units
q_o, oil Rate	1020	STB/D
q_w, water rate	0	STB/D
q_g, gas rate	306	MSCF/D
GLR	300	SCF/STB
Well Length, L	6792	ft
r_{ti} (inside tubing radius)	0.9075	in
r_{to} (outside tubing radius)	1.1875	in
r_{ci} (inside casing radius)	2.506	in
r_{co} (outside casing radius)	2.75	in
r_{wb} (well bore radius)	3.75	in
Heat transfer coefficient between the well bore and the formation, U	156.55	BTU/D-ft^2-F
Well roughness	0.001	ft
oil heat capacity, C_{po}	0.485	BTU/lbm-F
oil API	58	
Inclination to the horizontal, θ	90	
Rock thermal Properties		
Thermal rock conductivity (K_e)	33.6	BTU/D-ft-F
Heat capacity of rock	0.21156	BTU/lbm-F
Geothermal Gradient (G_T)	0.0274	F/ft
Temperature of the earth at the bottom hole of the well (T_{eibh})	237.2	F
Reservoir Properties		
Permeability (homogenous reservoir), K	200	md
thickness of the producing layer, h	20	ft
drainage radius, r_e	0.62	ft
oil formation volume factor, B_o	0.91	BBL/STB
Simulation Time, t	168	hr

Figure 2.5 shows the comparison of all the eight models with respect to the simulation results, all the models shows good agreement except for Sagar and Modified Sagar models due to the correlation used by Sagar[3] which might be not working for this case as the comparison was with Eclipse results not with a real data as this correlation was

developed from a real data or it might be the data used in this example are beyond the data base from which this correlation was developed.

Figure 2.6 shows the point-by-point comparison with Eclipse results for all the models except Sagar and modified Sagar as they both show high error compared to the other models. This figure shows the plot of the error between each model and simulation results versus depth, as it is seen from figure 2.6 that model 3 and 4 give less error compared to the other models less than 0.3 F difference from the simulation results for the distance close to the producing layer about 600 ft (at depth of 6192 ft).

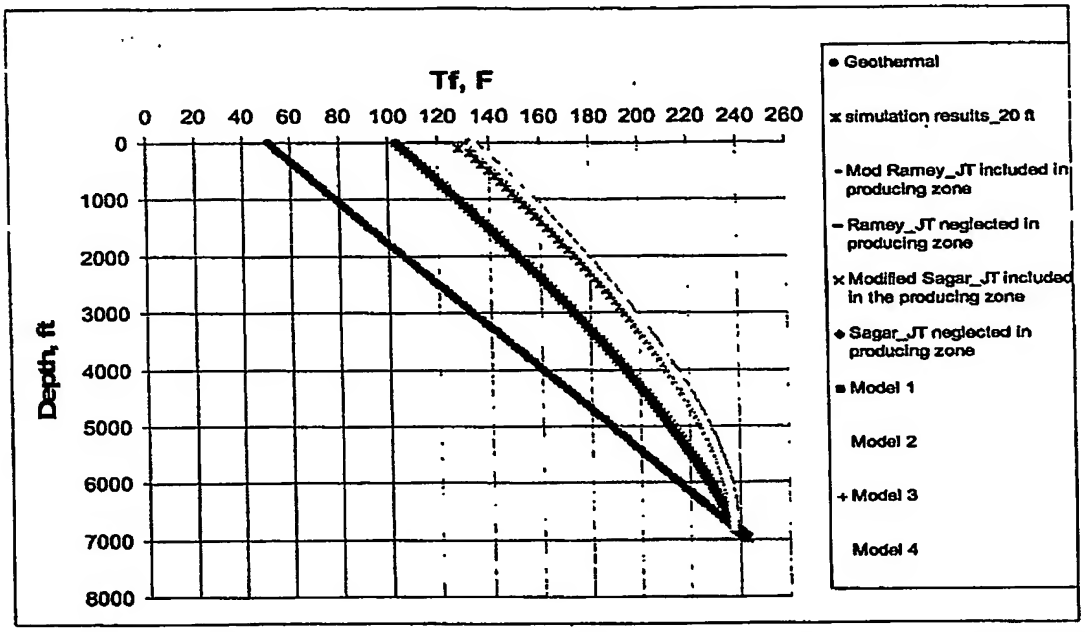

Fig. 2.5: Comparison of the eight analytical forward models with the numerical model (Eclipse 300, thermal option)

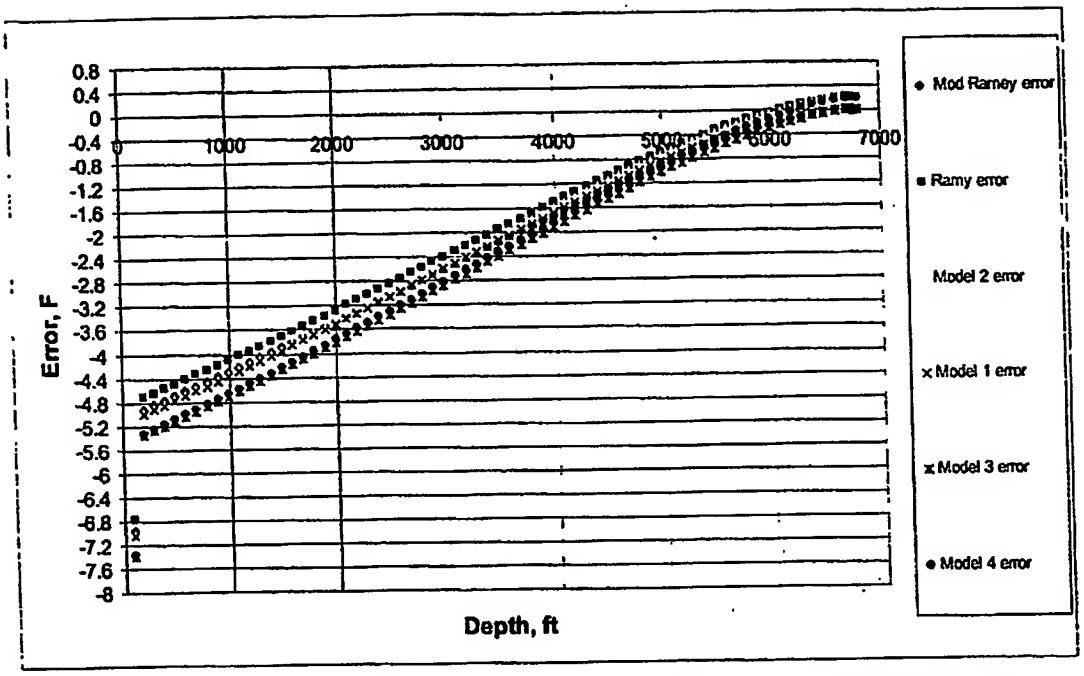

Fig.2.6: Error Comparison of the all the models except Sagar and Modified Sagar

Above the 6192 ft depth, models 3 and 4 gave higher error compared to the other models about 7 F difference from the simulation results at the surface and about a maximum of 0.6 F difference from the model of least error. The main reason that model 3 and 4 gave good results near the producing interval compared to the simulation is that gas holdup is still very small so the assumption of single phase liquid is holding, also the assumption of constant friction loss is reasonable whenever the gas holdup is very small which is the case near the producing interval. While at far distance from the producing interval the gas holdup is increasing and the assumption of constant friction loss and single phase liquid production does not hold anymore that is why model 3 and 4 are not giving good results at higher distance from the producing interval.

As we are interested only on the temperature analysis near the producing zones as there is a high chance to have a high liquid holdup and the assumption of liquid phase can be achieved so model 3 and 4 are the best candidates. Since as seen from Fig. 2.6 that the difference between model 3 and 4 are small and could be neglected, so model 4 is selected in order to reduce the uncertainty of imperfect knowledge about the reservoir properties like the type of the flow regime, permeability, drainage radius, reservoir thickness, etc.....

Chapter 3

TEMPERATURE FORWARD MODELING IN TWO LAYERS PRODUCTION WELLS

The objective of this chapter is to extend the temperature forward modeling derived in the previous chapter to be applied for two or multi-layers production wells for both single and two-phase liquid production. So, the first part of this chapter will concern on the way of extending model 4, which was derived from Eq. 2.43 by neglecting the Joule Thomson coefficient in front of the producing zone to be applied for the two layers production and the second part is to give the way of extending the forward model to two phase liquid two layers production wells.

[3.1] Temperature Forward Modeling for single-phase liquid, two layers production wells

Figure 3.1 shows a thermal nodal analysis sketch for two layers, single-phase liquid production wells.

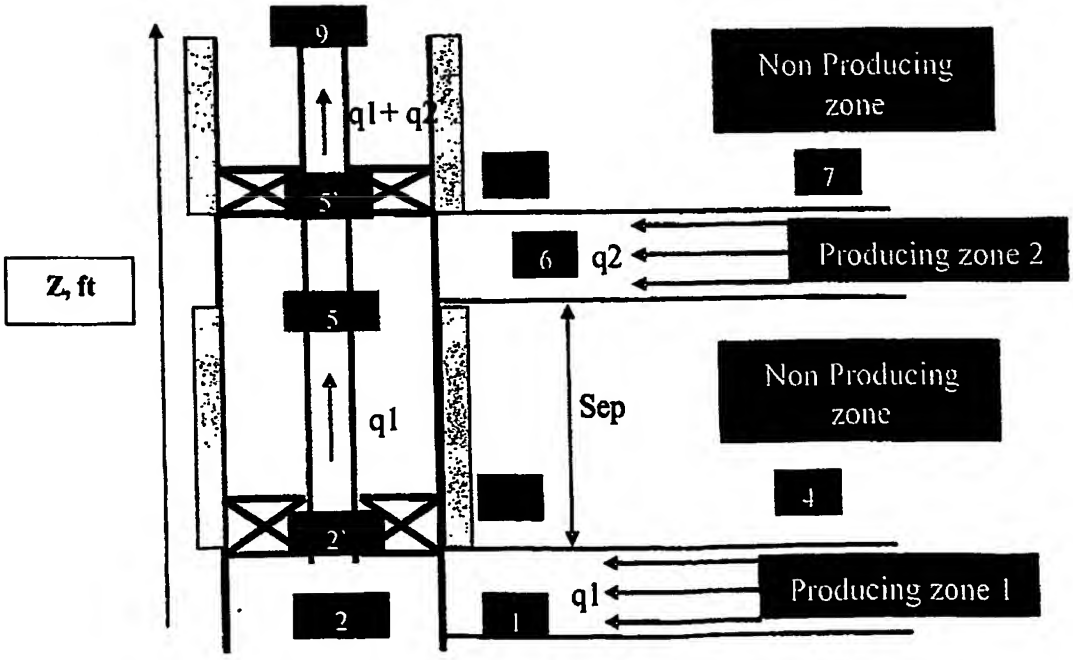

Fig. 3.1: Nodal Analysis for two layers, single-phase liquid production wells

The only difference between the single layer and the two layers production is in the nodal analysis between nodes 5-5`, nodes 8-7, and nodes 5`-9, also there is a minor change between nodes 2`-5. The main differences between the single and the two layers production will be mentioned for each of these nodes.

[3.1.1] Node 2`-5

The ordinary differential equation given across these nodes for the single layer production, Eq. 2.42, is the same as that used for the two layers production however the boundary condition that will be used is more general such as: $T_{fD}(z_D = z_{dbh}) = T_{fdbh}$

This general boundary condition allow us to handle the two or multi layers production cases as the temperature at node 5` should be corrected due to the mixing between the two streams and also due to the change of the rate from q_1 to q_1+q_2, so in this case as if we are dealing with the well as consisting of different sections each has the same equation but different boundary condition depending upon the temperature of the previous section.

The solution of Eq. 2.42 using the above general boundary condition has been done using **Mathematica** and the solution is as follows:

$$T_{fD} = \frac{1}{A_D\, T_{fbh}} \cdot \left[e^{-A_D z_{dbh}} \cdot \begin{pmatrix} e^{A_D z_{dbh}} \cdot (A_D\, T_{eibh} - G_T \,\mathrm{Sin}\theta\, (A_D\, z_D\, L + L) - T_{fbh}\, \phi_D) + \\ e^{A_D z_D} \cdot (-A_D\, T_{eibh} + A_D\, T_{fbh}\, T_{fdbh} + G_T \,\mathrm{Sin}\theta\, (A_D\, z_{dbh}\, L + L) + T_{fbh}\, \phi_D) \end{pmatrix} \right] \quad \text{.....(3.1)}$$

Where, T_{fdbh} is the temperature of entry and z_{dbh} is the depth measured from the bottom of the well at the entry level. Eqs. 2.38 and 2.39 are used to convert the dimensionless temperature profile obtained from Eq. 3.1 to the real domain.

[3.1.2] Node 5 - 5`

The modeling between node 5 and 5` is very similar to that between node 2 and 2` for the single layer production presenting in the previous chapter in that both mass and energy balance are applied, also the assumptions used between node 2 and 2` are the same as between node 5 and 5` except the last assumption where the heat capacity of the two streams are not the same and also the mixing rates are not equal.

Similarly, by dividing the producing zone into equal intervals, each interval producing equal rate. The number of divisions depends upon the number of temperature measurements in the producing zone and by applying a macroscopic mass and energy balance[2] due to the mixing of two streams from the upper producing zone and the total rate obtained from the lower zone, we can get the temperature at any interval inside the producing zone using the following derived equation:

$$T_{f(i)} = \frac{\left[q_1 + (i-1)\cdot(\frac{q_2}{n})\right] C_{p(i)} T_{f(i-1)} + \frac{q_2}{n} C_{p2}\, T_{ei}}{(q_1 + (i-1)\cdot\frac{q_2}{n}) C_{p(i)} + \frac{q_2}{n} C_{p2}} \qquad \text{.....(3.2)}$$

Where, i = 1, 2,.....n (n is the number of divisions or the number of temperature measurements inside the upper producing zone)

$T_{f(i)}$: is the temperature at each interval inside the producing zone, $T_{f(0)}$ is the well bore temperature at node 5.

C_{p2}: is the specific heat capacity of the fluid in the upper producing zone,

q_1, q_2 : is the total production from the lower zone and upper zone respectively

$C_{p(i)}$: is the specific heat capacity at each interval inside the producing zone and is calculating as a rate weighting average according to the following equation:

$$C_{p(i)} = \frac{\left[q_1 + (i-1)\cdot(\frac{q_2}{n})\right] C_{p(i-1)} + \frac{q_2}{n} C_{p2}}{\left[q_1 + (i)\cdot\frac{q_2}{n}\right]} \qquad \text{.....(3.3)}$$

Where, i = 1, 2, ...,n and $C_{p(0)} = C_{p1}$ which is the specific heat capacity of the fluid produced from the lower zone, which is constant through the section between node 2` and 5.

At node 5`,

$$T_{5'} = T_{f(n)} \qquad \text{.....(3.4)}$$

Also, $C_{p5'} = C_{p(n)}$ .....(3.5)

It should be noted that unlike Eq. 2.11, which is used to model the temperature from the lower producing interval (node 2-2`), Eq. 3.2 and 3.3 are rate dependent, however, it should be mentioned also that as the total rate from the two producing zones are null or very close to zero, Eq. 3.2 and 3.3 will blow up, so a condition should be imposed such

that at very small or zero rates from the two producing zones, the temperature should be equivalent to the geothermal temperature so that to honor the physics of the problem.

Also, it should be noted that T_{ei} in Eq. 3.2 could be corrected due to the pressure drop across the perforation in a similar way that has been described in the previous chapter by using Eqs. 2.8 and 2.9 or the Joule Thomson effect can be neglected and T_{ei} will be directly the geothermal temperature as was found from the previous chapter that the correction due to the Joule Thomson effect in front of the producing zone could be neglected.

In case of synthetic examples, and to simplify the calculation, we can consider that we have only one temperature measurement at the top of the upper producing interval so that i =1 and n = 1 in Eqs. 3.2 and 3.3 so that we can get $T_{5'}$ by knowing T_5 and T_6

[3.1.3] Node 8 – 7

The same equation described in the previous chapter between node 3 and 4 can be used between node 8 and 7 but the flow rate is the total rate from the two producing zones.

[3.1.4] Node 5` – 9

Eq. 3.1 can be used to describe the temperature profile between node 5` and 9 by using the total rate ($q_1 + q_2$) instead of $q_1$. Also, $C_p$ between node 5` and 9 is equal to $C_{p5'}$ as calculated from Eq. 3.5.

[3.2] Temperature Forward Modeling for two-phase liquid, two layers production wells

Fig. 3.2 shows the nodal analysis sketch for two phase two layers production, where the two phases are oil-water (liquid), so that the forward model derived before will be applicable.

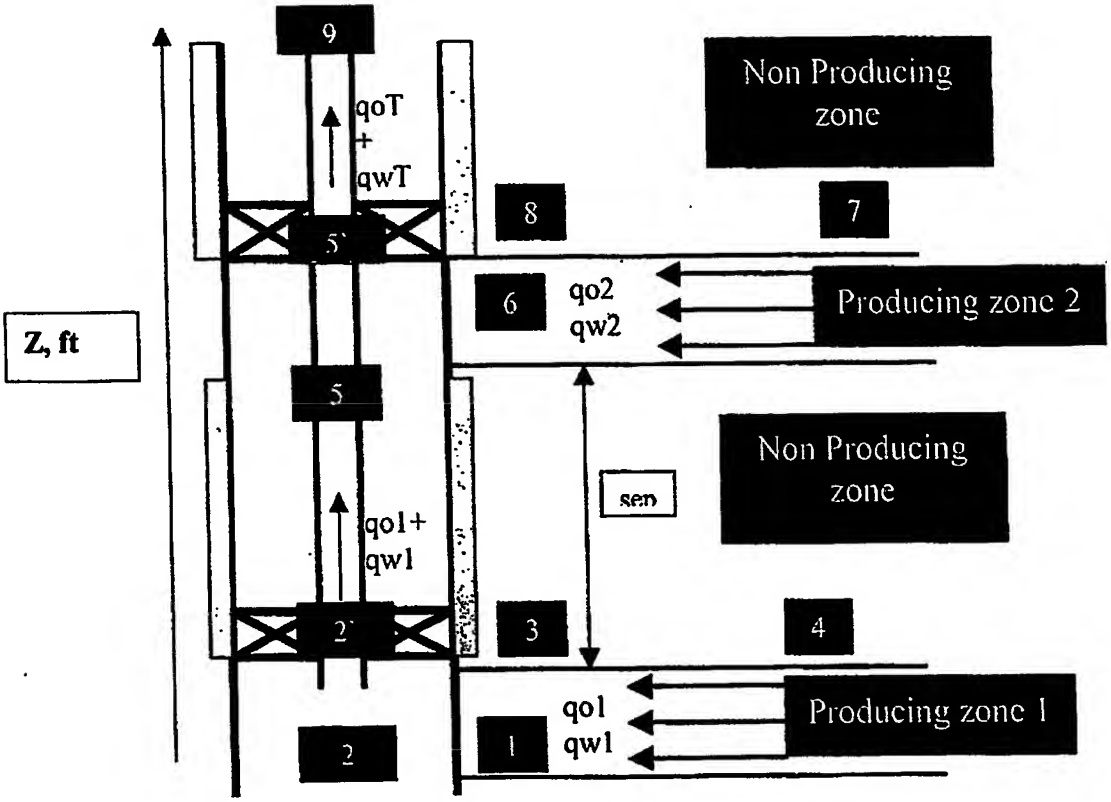

Fig.3.2: Thermal Nodal analysis for two phase, two layers production well

The extension of the modeling to two-phase flow depends upon recalculating the parameters of the modeling for the two-phase flow. The equation for each parameter will differ depend upon the nodal location, thus, the equation for each parameters will be given between each node with a special reference to the equation used in the temperature modeling.

It should be noted that in the non producing zone as there is no fluid flow, only heat energy flow, so the change from single phase to two phase flow will not affect the temperature modeling between nodes 3 and 4 and node 8 and 7.

Also, it should be mentioned that the correction of the temperature due to the pressure drop in front of the producing interval is neglected otherwise we need to have and additional inputs to the model which are the relative permeability and the capillary pressure which will increase the uncertainty of the modeling.

[3.2.1] Node 2-2`

As seen from Eq. 2.11, that the temperature modeling between these two nodes depends only on the geothermal temperature, which does not depend upon the production phase, so the temperature modeling between node 2 and 2` is the same as for single-phase flow.

[3.2.2] Node 2`- 5

Eq. 3.1 is used to get the temperature distribution between these two nodes. The parameters with its equation that are required to be obtained due to the two-phase flow are as follows:

1- For A_D calculation the parameters required are: w_t and C_p, w_t is calculated using Eq. 2.22a where q_w is substituted by q_{w1} and q_o is substituted by q_{o1}, while Cp between nodes 2` and 5 is calculated according to the following equation:

$$C_{p1} = \frac{C_{po} \cdot q_{o1} + C_{pw} \cdot q_{w1}}{q_{o1} + q_{w1}} \qquad \text{.....(3.6)}$$

2- For the ϕ_D parameters the parameters that are required to be obtained for the two-phase flow are: q, C_p, μ, ρ. Those parameters can be obtained as follows:

i- $q = q_1 = q_{o1} + q_{w1}$ .....(3.7)

ii- C_p is calculated as given by Eq. 3.6

iii- $$\mu = \mu_1 = \frac{\mu_o \cdot q_{o1} + \mu_w \cdot q_{w1}}{q_{o1} + q_{w1}} \qquad \text{.....(3.8)}$$

iv- $$\rho = \rho_1 = \frac{\rho_o \cdot q_{o1} + \rho_w \cdot q_{w1}}{q_{o1} + q_{w1}} \qquad \text{.....(3.9)}$$

[3.2.3] Node 5 – 5`

Eq. 3.2 and 3.3 are used to calculate the temperature between these nodes by substituting q_1 by ($q_{o1} + q_{w1}$) and q_2 by ($q_{o2} + q_{w2}$), C_{p2} is calculated from the following equation

$$C_{p2} = \frac{C_{po} \cdot q_{o2} + C_{pw} \cdot q_{w2}}{q_{o2} + q_{w2}} \qquad \text{.....(3.10)}$$

[3.2.4] N de 5`– 9

Same as between node 2`- 5 mentioned before but with the following differences:

i- For w_t, it is calculated using Eq. 2.22a, where $q_w = q_{wT} = q_{w1} + q_{w2}$ and $q_o = q_{oT} = q_{o1} + q_{o2}$

ii- For C_p, it is calculated using the following equation

$$C_{pM} = \frac{C_{po} \cdot (q_{o1} + q_{o2}) + C_{pw} \cdot (q_{w1} + q_{w2})}{q_{o1} + q_{o2} + q_{w1} + q_{w2}} = C_{p5} \qquad \text{.....(3.11)}$$

iii- For the ϕ_D calculation the parameters required to be calculated are:

$$q = q_{o1} + q_{w1} + q_{o2} + q_{w2} \qquad \text{.....(3.12)}$$

$$\mu = \frac{\mu_o \cdot (q_{o1} + q_{o2}) + \mu_w \cdot (q_{w1} + q_{w2})}{q_{o1} + q_{w1} + q_{o2} + q_{w2}} \qquad \text{.....(3.13)}$$

$$\rho = \frac{\rho_o \cdot (q_{o1} + q_{o2}) + \rho_w \cdot (q_{w1} + q_{w2})}{q_{o1} + q_{w1} + q_{o2} + q_{w2}} \qquad \text{.....(3.14)}$$

The extension of the temperature modeling to multi-layers two-phase flow is trivial as it is only an extension of the equations mentioned in this chapter and in the previous one.

Chapter 4

TEMPERATURE INVERSE MODELING WITH SYNTHETIC EXAMPLES

As the major objective of this study is to use the temperature forwarding modeling discussed in the previous two chapters as the forward tool and use it in inverting the temperature measurements inside the producing wells to allocate the rates from the producing layers. So, the main objective of this chapter is to give a short introduction about how we can do the inversion of temperature for rate allocation, test the applicability to invert the temperature for zonal allocation for a single phase production under different scenarios in order to pick the critical scenarios through which the inversion might or might not work. Then use these critical scenarios to study the accuracy of zonal allocation by introducing errors in the forward model parameters, and finally, testing the accuracy of the inversion for two phase production on the critical scenarios proposed before. So the organization of this chapter will be, first give a brief introduction about the inversion, second testing the inversion on different synthetic examples for single-phase two layers production, then show the accuracy of the inversion for the errors in the forward model parameters and finally testing the inversion for two phase two layers production wells.

[4.1] Inverse Temperature Modeling

Inversion in its broad meaning is to find the independent parameters in the forward model that minimize the error between the measured dependent parameter and the calculated dependent parameter from the forward model. So, it is an optimization problem where we want to minimize a certain objective function, which is the error between the measured and the calculated dependent parameters, by changing the independent parameters in a certain domain, or in other words changing the independent parameters according to specified constraints.

In this study, the dependent parameter is the temperature and the independent parameters are mainly the zonal rates or could be any other input parameters of the forward

modeling. Accordingly, the mathematical description of the optimization problem is as follows:

$$Min\ O(\mathbf{m}) = Min\left[\sum_{i=1}^{n_d}\left(T_i^{cal}(\mathbf{m}) - T_i^{obs}\right)^2\right] \quad \text{subject to } \{\text{any constaints on } \mathbf{m}\} \quad .....(4.1)$$

Where, **m:** is a vector of the independent parameters, mainly the zonal rates and some other input parameters.

There are many optimization algorithms in different books[11, 12] that can be used to find the zonal rate by minimizing the error between the temperature measured from DTS (Distributed temperature sensors) and the calculated temperature from the forward modeling discussed in the previous two chapters, however for simplicity and to make the analysis of DTS fast and easy to handle for the users, I used the optimization algorithm coded in Excel which is the "Generalized Reduced Gradient"[13] so that the user can do the analysis using Excel without any programming skill.

[4.2] Inversion Testing for Single-Phase Two Layers Producing Wells

The major concern of this part is to see whether the rate can be allocated by knowing only the temperature measurements in producing wells under different scenarios, the selection of these scenarios depends upon an early work[14] that shows that the main factors which affect the rate allocation are 1- temperature contrast between the two zones, 2- the production time, and 3- the amount of the flow rates. Accordingly eight different scenarios have been tested using synthetic examples for a single phase two layer producing well to see which is the most severe factor that has high effect on the rate allocation. Those scenarios are as follows:

1- Small rate from the lower zone (200 STB/D) and high rate from the upper zone (800 STB/D), low temperature contrast between the two producing zones (about 3 F, equivalent to a separation distance of 100 ft), and low production time (10 days).

2- Small rate from the lower zone (200 STB/D) and high rate from the upper zone (800 STB/D), high temperature contrast between the two producing zones (about 13 F, equivalent to a separation distance of 500 ft) and low production time (10 days).

3- Small rate from the lower zone (200 STB/D) and high rate from the upper zone (800 STB/D), low temperature contrast between the two producing zones (3 F, equivalent to a separation distance of 100 ft) and high production time (100 days).
4- Small rate from the lower zone (200 STB/D) and high rate from the upper zone (800 STB/D), high temperature contrast between the two producing zones (13 F, equivalent to a separation distance of 500 ft) and high production time (100 days).
5- High rate from the lower zone (800 STB/D) and low rate from the upper zone (200 STB/D), low temperature contrast between the two producing zones (3 F, equivalent to a separation distance of 100 ft) and low production time (10 days).
6- High rate from the lower zone (800 STB/D) and low rate from the upper zone (200 STB/D), high temperature contrast between the two producing zones (13 F, equivalent to a separation distance of 500 ft) and low production time (10 days).
7- High rate from the lower zone (800 STB/D) and low rate from the upper zone (200 STB/D), low temperature contrast between the two producing zones (3 F, equivalent to a separation distance of 100 ft) and high production time (100 days).
8- High rate from the lower zone (800 STB/D) and low rate from the upper zone (200 STB/D), high temperature contrast between the two producing zones (13 F, equivalent to a separation distance of 500 ft) and high production time (100 days).

Through all the above 8 scenarios, I used the input data given in Table 4.1 in addition to the rates, time and the information about the separation distance between the two zones to get a true temperature profile inside the producing well using the forward modeled developed in the previous two chapters. Then, starting with initial guess of zero or very small rates from the two producing zones, which is equivalent to assuming the initial guess is the geothermal temperature and assuming a perfect knowledge in the input data by using the same data set given in Table 4.1 in addition to the production time and the separation distance between the producing zones given in each scenario to do the inversion on only the true generated temperatures very close to the two producing intervals. So, the T_i^{obs} in Eq. 4.1 is the true generated temperature and T_i^{cal} is the calculated temperature from the forward model using the same input data that is used to

generate the true temperature but with different rates, which are very small rates for the initial guess and there is no constraint imposed during working in those scenarios.

Table 4.1: Input data for the synthetic examples of the different eight scenarios for single phase two layers production well

	Value	Units
Formation Thermal Properties		
Geothermal gradient, G_T	0.0274	F/ft
Thermal diffusivity, α	0.04	ft^2/hr
Thermal conductivity, K_e	33.6	BTU/D-ft-F
Bottom hole temperature, T_{eibh}	237.2	F
Fluid properties		
Oil API	58	API
Oil specific heat capacity, c_{po}	0.485	BTU/lbm-F
Oil viscosity, μ_o	1.06744	cp
Well Data		
Total length of the well, L (Depth of the lower zone)	6792	ft
Inside radius of the tubing, r_{ti}	0.9075	in
Outside radius of tubing, r_{to}	1.1875	in
Inside radius of the casing, r_{ci}	2.506	in
Outside radius of the casing, r_{co}	2.75	in
Well bore radius, r_{wb}	3.75	in
Annulus water thermal conductivity, K_{amw}	9.192	BTU/D-ft-F
Cementing material thermal conductivity, k_{cem}	96.5	BTU/D-ft-F
Tubing roughness	0.001	ft
Inclination angle to the horizontal, θ	90	Deg.

All the results from all the scenarios show the high ability to invert easily for allocating the rates from the two producing zones by knowing only the temperature profile very close to the producing intervals. Figure 4.1 shows the results from scenario 7, as it is found that this scenario took the largest number of iterations to converge, about 14 iterations using the generalized reduced gradient (GRG) coded in Excel and using only the points near the producing zones. In Fig. 4.1, the initial temperature profile is the temperature calculated from the forward model using very small rates as initial guess, the true temperature (considered as measured temperature) is the temperature generated from the forward

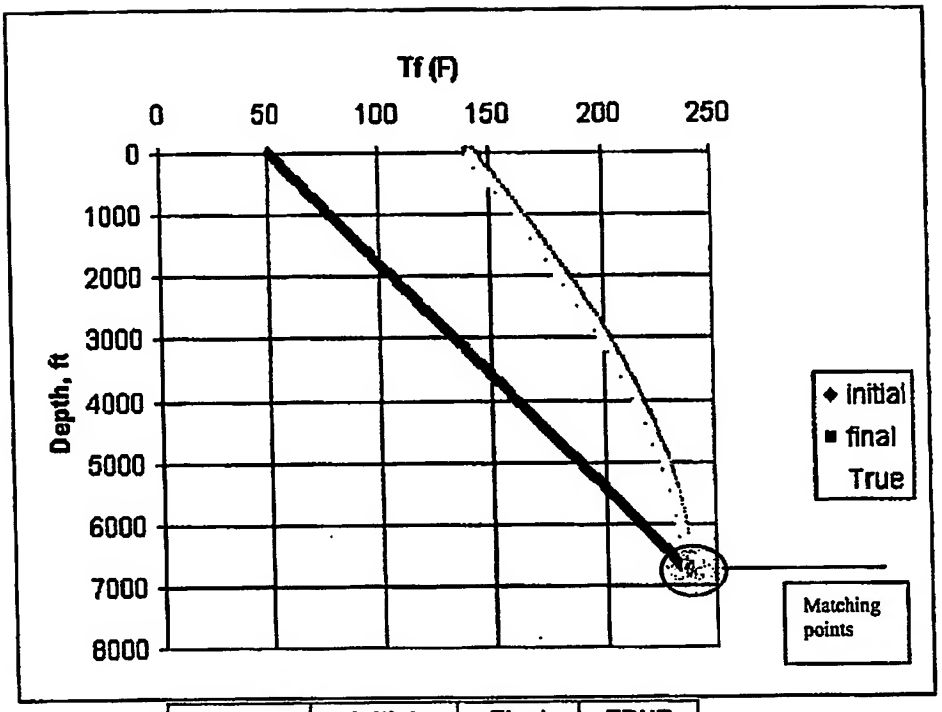

	Initial	Final	TRUE
qo1, STB/D	0.001	800.1194	800
qo2, STB/D	0.001	200.0314	200

Fig. 4.1: Scenario 7 results for rate allocation

model using the true rates and the other data mentioned in each scenario and the final temperature is the temperature at final iteration, also given in the Fig. 4.1 the initial, true and final rates from each zone. It should be noted that in the above synthetic examples for each scenario model 4 is used as the forward model, in which the Joule Thomson coefficient is neglected in front of the producing zones only. There are two things that have been done for the synthetic examples for those 8 scenarios and also for all the synthetic cases that will be presented in this chapter just to simplify the calculations. First, there is no temperature points in front of the lower producing zone, so that node 2 and 2` are considered on node 2`, second, there is only one temperature point in front of

the upper producing zone and its location is at the top of the upper zone, which is at node 5`.

From the above testing of the inversion for the different 8 scenarios, it was found that the only scenarios that show a big difference in the number of iterations are the scenarios that contain the high and low temperature contrast compared to the minor difference due to the time and rate changes. So, in the next part I will study the accuracy of the rate allocation by introducing error in the model parameters for the scenarios that have high and low temperature contrast. The scenarios selected for this study are scenarios 7 and 8 as they both show higher number of iterations to converge compared to the others.

[4.3] Testing the Accuracy of Rate Allocation for Single-Phase Two Layers Producing Wells

The major concern of this part is to show how the uncertainties in the forward model parameters affect the rate allocation from the two producing zones. Nine cases have been studied to show how the effect of the errors in the parameters affecting the rate allocation from the two producing zones. The forward model used is Model 4 and the effect of each case has been studied for scenarios 7 and 8. Table 4.2 and Fig. 4.2 show the different cases that have been studied to test the accuracy of the rate allocation for the low and high temperature contrast scenarios.

It should be noted that the input data used to generate the true temperature for the nine cases are the same as that given in Table 4.1 and scenarios 7 and 8. So, case one, where we assume a perfect knowledge of the input data, is exactly the same as the results obtained from scenarios 7 and 8, while in the other cases, error has been introduced to most of the model parameters to see its effect in the accuracy of the zonal allocation. Case 9 shows a combined error of some of the parameters. Also, it is important to mention that that the objective function used in those nine cases are the same as in Eq. 4.1 using only the points near the producing zones and without constraint. However for cases 8^* and 9^* the total rate has been introduced as constraint in the optimization problem and also using the points very close to the producing zones.

Table 4.2: *Cases description and errors in rate allocation due to errors in model parameters for low and high temperature contrast*

Cases	Conditions	Error in q1, %		*Error in q2, %*		*Comments*
		Low temp. Contrast	High temp. Contrast	Low temp. Contrast	High temp. Contrast	
1	Perfect information about all the parameters	0.0027	0.00103	0.0074	0.00162	
2	200% error in the roughness of the tubing	4.51	2.67	4.14	2.8	High error is used for the roughness as it is the only parameters that has a high uncertainty
3	10% error in oil heat capacity	4.68	9.15	4.66	9.05	
4	10% error in oil specific gravity	0.19	1.67	0.06	1.66	
5	10% error in the production time	0.5	0.5	0.7	0.7	
6	10% error in the overall heat transfer coefficient	2.94	4.08	2.93	4.06	
7	10% error in the geothermal gradient	8.3	9.2	3.7	3.8	
8	Error in temperature measurements (normal distribution of mean zero and S.D of 0.1), in addition using only two digits precision for the temperature measurements	74.5	8.18	74.2	15.18	
8*	Case 8, including total rate as constraint	5	0.7	20.5	3	By including the total rate as constraint in the objective function, the results of the error in the rate allocation has been improved
9	Mixing of all the above cases	69.3	1.11	72.4	18	
9*	Case 9, including total rate as constraint	2.45	3.7	9.8	14.8	By including the total rate as constraint in the objective function, the results of the error in the rate allocation has been improved

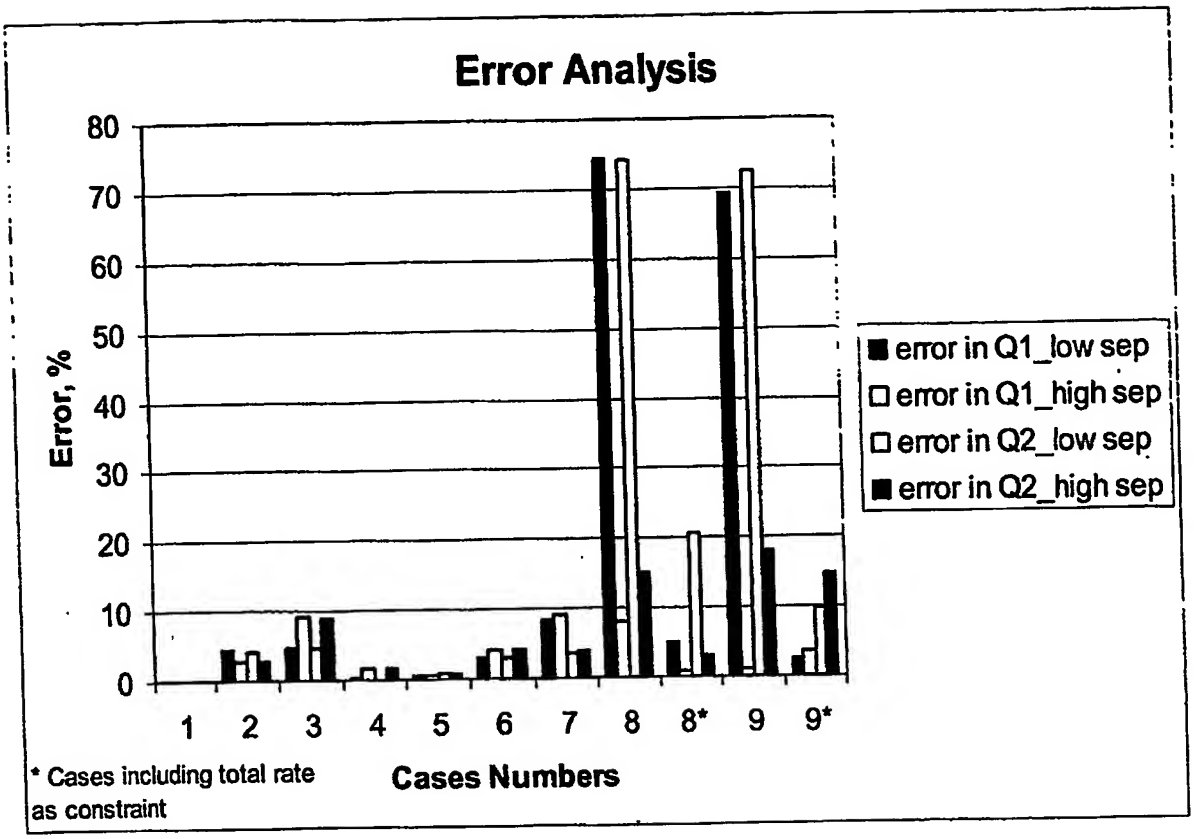

Fig. 4.2: Error analysis of rate allocation for error in the model parameters

From the above results it was found that:

1- In all the cases that have error of 10 % in its parameters, the rate allocation from the two producing zones show error less than 10 % except for cases 8 and 9. Case 8, where errors in the temperature measurements has been generated which ranges from –0.3 to 0.3 F, while case 9 including all the error in the parameters in one single case

2- Improvement in the rate allocation has been shown after including total rate as constraint in the objective function. Also, another observation is that case 9, which includes all the error in the parameters shows approximately good results compared to case 8, this might be due to that some errors in the parameters have opposite effects which leads to a kind of improvements in the rate of allocation when taking all the errors in the parameters in one case.

[4.4] Inversion Testing for Tw -Phase Tw Layers Producing Wells

The target of this part is to test the inversion for the case of two phase two layers production to see whether it is possible to allocate the rate under perfect knowledge of input parameters or not. The scenarios that will be studied are scenarios 7 and 8 with and without imposing the total rate for each phase as constraint in the objective function. The true temperature will be generated similarly as have been done before using the true rates from the two producing zones to be as follows: q_{o1} = 300 STB/day, q_{o2} = 200 STB/day, q_{w1} = 350 STB/day, and q_{w2} = 300 STB/day. Also the time and the separation between the zones will be the same as that presented in scenarios 7 and 8, while the other input parameters will be given in Table 4.3.

Table 4.3: **Input data for the synthetic examples of the two phase two layers production well for scenarios 7and 8**

	Value	Units
Formation Thermal Properties		
Geothermal gradient, G_T	0.0274	F/ft
Thermal diffusivity, α	0.04	ft^2/hr
Thermal conductivity, K_e	33.6	BTU/D-ft-F
Bottom hole temperature, T_{eibh}	237.2	F
Fluid properties		
Oil API	30	API
Oil specific heat capacity, c_{po}	0.485	BTU/lbm-F
Oil viscosity, μ_o	1.06744	cp
Water specific gravity, γ_w	1	
Water specific heat capacity, C_{pw}	1	BTU/lbm-F
Water viscosity	0.31	cp
Well Data		
Total length of the well, L (Depth of the lower zone)	6792	ft
Inside radius of the tubing, r_{ti}	0.9075	in
Outside radius of tubing, r_{to}	1.1875	in
Inside radius of the casing, r_{ci}	2.506	in
Outside radius of the casing, r_{co}	2.75	in
Well bore radius, r_{wb}	3.75	in
Annulus water thermal conductivity, K_{anw}	9.192	BTU/D-ft-F
Cementing material thermal conductivity, k_{cem}	96.5	BTU/D-ft-F
Tubing roughness	0.001	ft
Inclination angle to the horizontal, θ	90	Deg

Table 4.4 and Fig. 4.3 show the result of the inversion for the two scenarios starting by very small values of the rates as an initial guess and taking into consideration that we are using only the points that are close to the producing interval in the optimization.

Table 4.4: Test of the inversion for two-phase two layers production for high and low temperature contrasts between the zones with and without imposing total phase rates as constraint

	q_{o1} Error, %	q_{o2} Error, %	q_{w1} Error, %	q_{w2} Error, %	q_{o1} Error, %	q_{o2} Error, %	q_{w1} Error, %	q_{w2} Error, %
	High Temperature Contrast				**Low Temperature Contrast**			
Without Total rate	45.2	24.3	16.9	6	44.75	30.31	15.65	6.6
With total rate	0.4	0.6	0.17	0.2	10.2	15.3	4.25	4.96

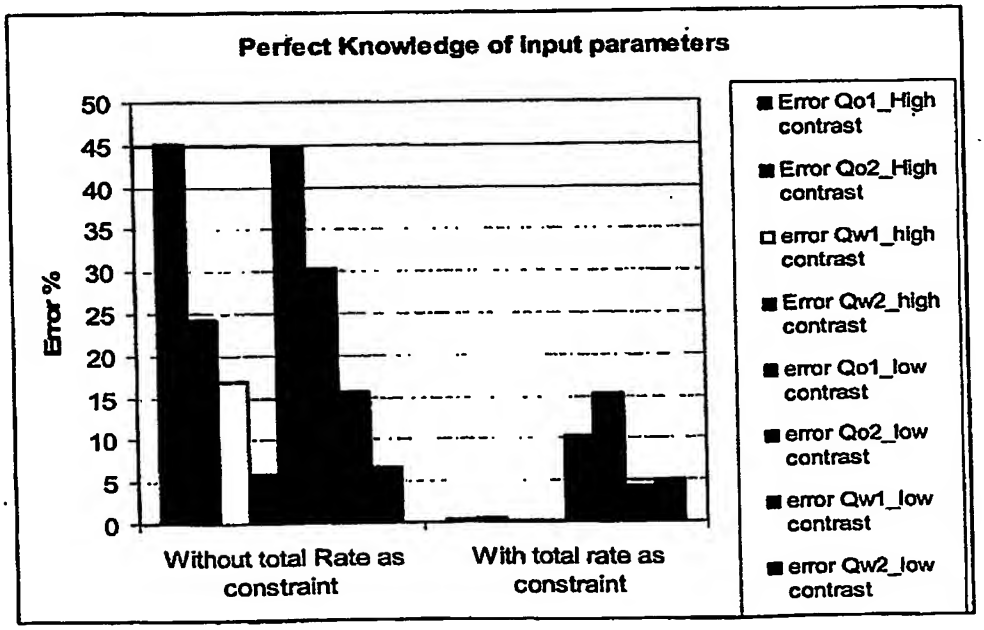

Fig. 4.3: Error in rate allocation for high and low temperature contrasts between the zones under with and without imposing total rate as constraint for a perfect knowledge of input parameters

From the results of the above study, it was shown that imposing the total rate of each produced phase improves the accuracy of the rate allocation for the high temperature contrast but it does not do a good job for the low one, however we assumed a perfect knowledge of the input data. That is why it is very difficult to allocate the rates for the two phase production for imperfect knowledge of the input data as to accurately allocate the rates, any extra information other than total rate for each phase is required to make the problem well constraint and not to be trapped in any local minima as was done in the above synthetic examples for the low temperature contrast with and without total phase rate as constraint and in the high temperature contrast without total phase rate constraint.

Chapter 5
FIELD EXAMPLE

The primary objective of this chapter is to test the forward modeling with respect to real field data and the secondary objective is to see how the inversion will work in handling true data other than the synthetic examples that was mentioned in the previous chapter and also to check whether the findings from the synthetic examples are reasonable or not. So, this chapter is organized as follows: the first part will concern with the data description and the second part is data analysis, which is devoted to analyze the data and discuss the results.

[5.1] Data Description

The field example is taken from Bugan-07 well, which is a 4 zone intelligent well completion with 3 ICV's to allow any or all of the producing intervals to be flowed at the same time, the completion for this well is given in Fig. 5.1. In March 13, 2003 well testing has been done to test the flow from the middle two zones while the other two zones are closed, the test shows a total oil production of 769 m^3/day (4836.5056 bbl/day), and total water production of 236 m^3/day (1484.2852 bbl/day). Fiber optic line has been installed in the completion to measure the temperature inside the well bore and also information about the geothermal gradient has been given for this area. Fig. 5.2 shows the temperature recording inside the well bore, the geothermal temperature for the section that is closed to the two producing zones as was mentioned before that we are only interested on the data very close to the producing intervals and also the perforation interval for each zones. As seen from Fig. 5.2 that the temperature data are very rough, so I smoothed the data using a moving average statistical technique every 10 measurement points and the smoothed temperature is also plotted in Fig. 5.2, the smoothed data will then be used for our analysis. It should be noted that Bugan 07 well is a deviated well and the average inclination angle with horizontal for the section that we are interested on is 46.36°. From the geothermal gradient, the inclination angle, and the bottom hole measured temperature, it was found that the temperature contrast between the two zones is about 7 F, which is an intermediate case compared to the synthetic examples that have

been showed before, where we showed cases of 13 F and 3 F temperature contrast between the producing zones.

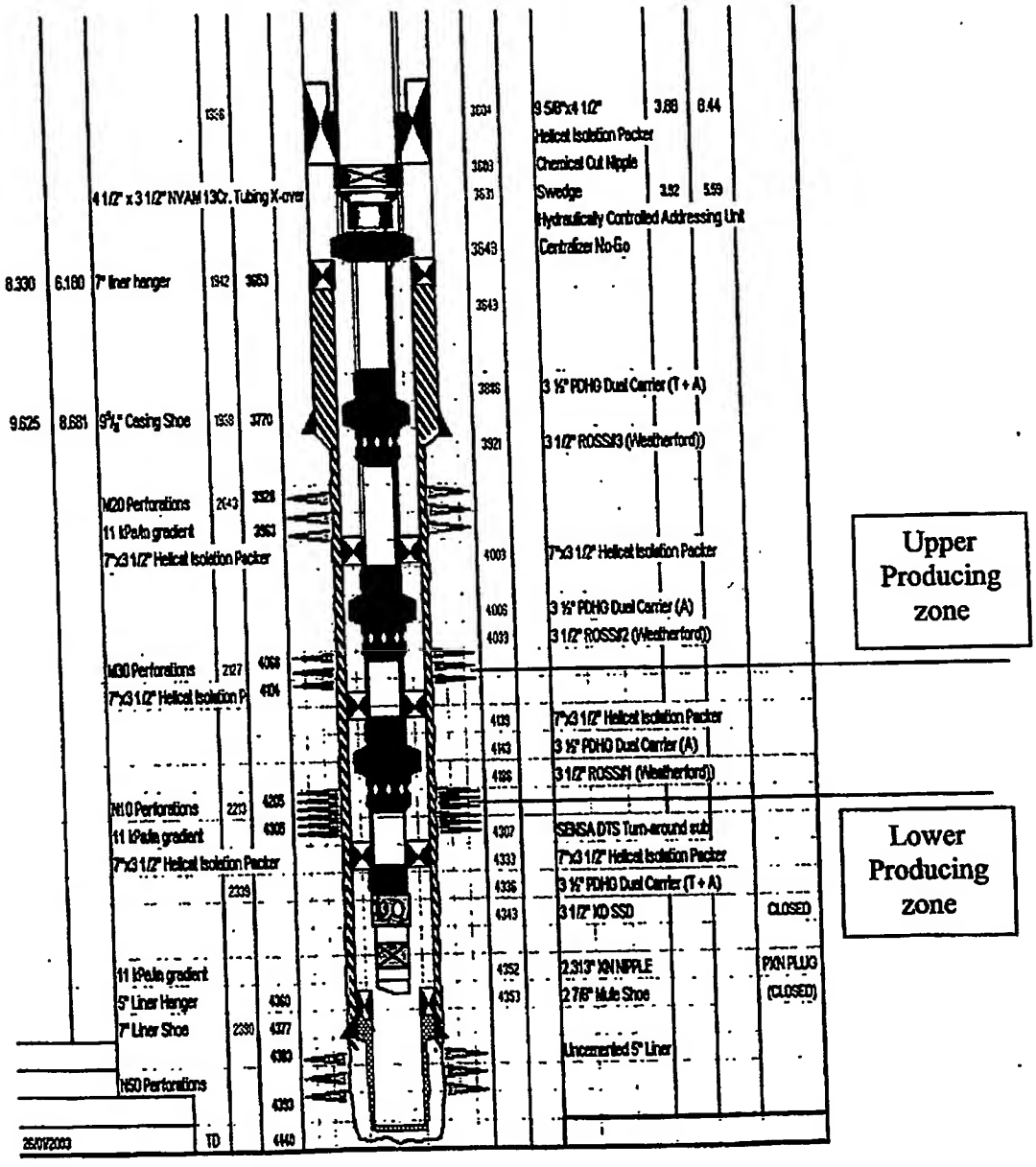

Fig. 5.1: Completion of Bugan 07 Well

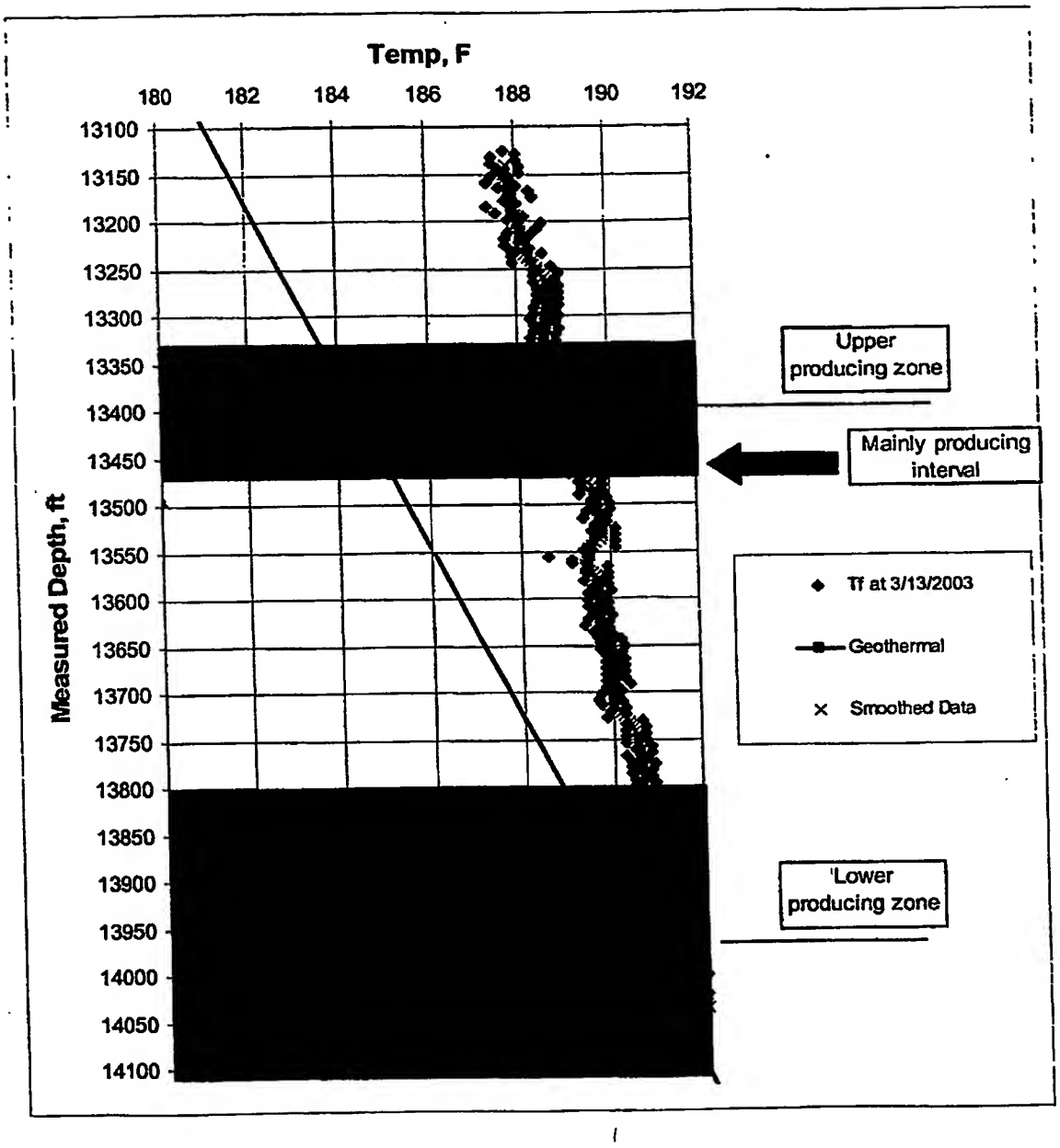

Fig. 5.2: Temperature measurement inside the well bore, geothermal temperature, smoothed temperature, and the perforation intervals for each producing zones

[5.2] Data Analysis

From a quick look qualitative interpretation of the temperature data whether the smoothed or the rough one, it could be easily noticed that not all the perforated interval from the upper zone is produced as we can see that only small portion of the upper producing interval has a decline in temperature due to the mixing of the fluid of low temperature from the upper zone and high temperature from the lower zone which cause this reduction in temperature, while the other portion of the zone does not show this reduction.

Table 5.1 shows the data used for the forward modeling of temperature of this field case. The data in **bold** are the data that there are no information about them, so I add those data as parameters in the inversion to be changed to match the measured temperature. Values of the data given in the table are the values after inversion. For the inverse modeling to get the rates from each zone, I used the same objective functions given in Eq. 4.1, where the vector (**m**) are the rates from each zones and the input data given in Table 5.1, and the constraints are given in Table 5.2.

It should be mentioned that the main difference between the input data for the synthetic cases, Table 4.3, and for the field case, Table 5.1, is that in field case, there are number of temperature measurements inside each producing zone, so the information about those numbers should be given, while in case of synthetic examples, we assume that there is no measurement points inside the producing zones, so no additional information about the number of temperature measurements are required. In addition, Table 5.1 needs information like the formation density and specific heat capacity to calculate the formation diffusivity, while in the synthetic examples; we just input the formation diffusivity, just to simplify the calculation.

Also, the bounded constraints given in Table 5.2 are taken from the literature[4, 15] so that there is no unrealistic results will be obtained to the parameters entered in the optimization as a result of inversion.

Table 5.1: Input Data for the field example

	Value	Units
Formation Thermal Properties		
Geothermal gradient, G_T	0.01538	F/ft
Formation Density, ρ_e	**176.85**	**Lbm/ft^3**
Formation heat capacity, C_e	**0.7**	**BTU/lbm-F**
Thermal conductivity, K_e	**96**	**BTU/D-ft-F**
Bottom hole temperature, T_{elbh}	191.91	F
Fluid properties		
Oil API	30	API
Oil specific heat capacity, c_{po}	**0.4**	**BTU/lbm-F**
Oil viscosity, μ_o	1.06744	cp
Water specific gravity, γ_w	1	
Water specific heat capacity, C_{pw}	**0.477**	**BTU/lbm-F**
Water viscosity	0.31	cp
Well Data		
Total length of the well, L (Depth of the lower zone)	14089.46	ft
Inclination to the horizontal, θ	46.36	Deg.
Inside radius of the tubing, r_{ti}	1.5	in
Outside radius of tubing, r_{to}	1.75	in
Inside radius of the casing, r_{ci}	2.75	in
Outside radius of the casing, r_{co}	3.5	in
Well bore radius, r_{wb}	4.5	in
Annulus water thermal conductivity, K_{anw}	**10**	**BTU/D-ft-F**
Cementing material thermal conductivity, k_{cem}	**94.23**	**BTU/D-ft-F**
Tubing roughness	0.001	ft
No. of temperature measurements in the lower producing zone	90	Meas.
No. of temperature measurements in the upper producing zone	12	Meas.
Depth to the top of the upper producing zone	13428	ft
Depth to the bottom of the upper producing zone	13464	ft
Depth to top of the top of the lower producing zone	13795	ft
Production time	840	days

Table 5.2: The constraints for the model parameters

Parameters	Inequality	Value	Units
q_{o1}	>=	0	STB/D
q_{o2}	>=	0	STB/D
q_{w1}	>=	0	STB/D
q_{w2}	>=	0	STB/D
ρ_e	>=	75	lbm/ft3
ρ_e	<=	185	lbm/ft4
C_e	>=	0.1	BTU/lbm-F
C_e	<=	0.7	BTU/lbm-F
K_e	>=	10	BTU/D-ft-F
K_e	<=	96	BTU/D-ft-F
K_{amw}	>=	8	BTU/D-ft-F
K_{amw}	<=	10	BTU/D-ft-F
C_{po}	>=	0.4	BTU/lbm-F
C_{po}	<=	1	BTU/lbm-F
C_{pw}	>=	0.4	BTU/lbm-F
C_{pw}	<=	1	BTU/lbm-F
q_{oT}	=	4836.5056	STB/D
q_{wT}	=	1484.2852	STB/D

Fig. 5.3 shows the comparison between the measured and the modeled temperature after the inversion. The rate allocation from each zone were found to be as follows: $q_{o1} = 2850$ bbl/day, $q_{o2} = 1986.5$ bbl/day, $q_{w1} = 1174.11$ bbl/day, $q_{w2} = 310.17$ bbl/day

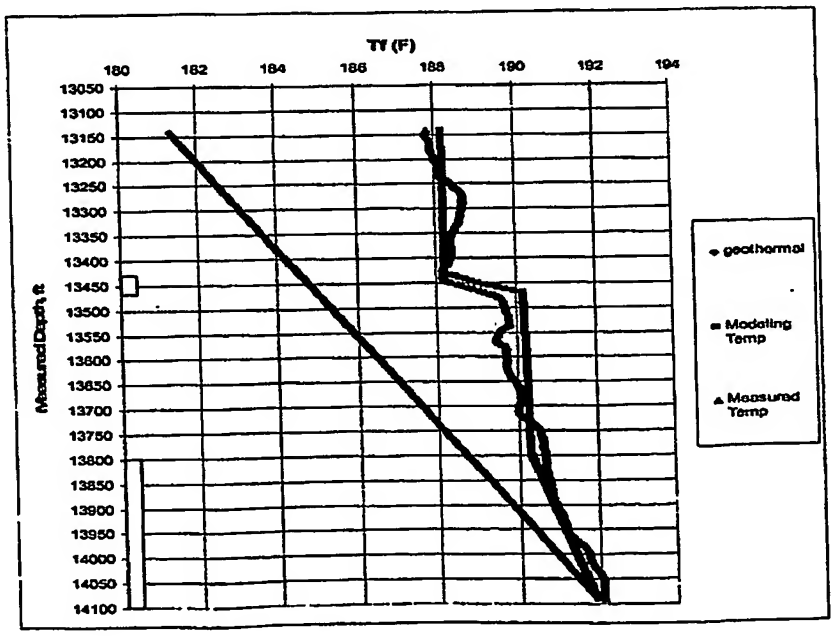

Fig 5.3: Comparison between modeled and measured temperature

Fig. 5.4 shows the absolute errors between the modeled and the measured temperature across the section of the well under study,

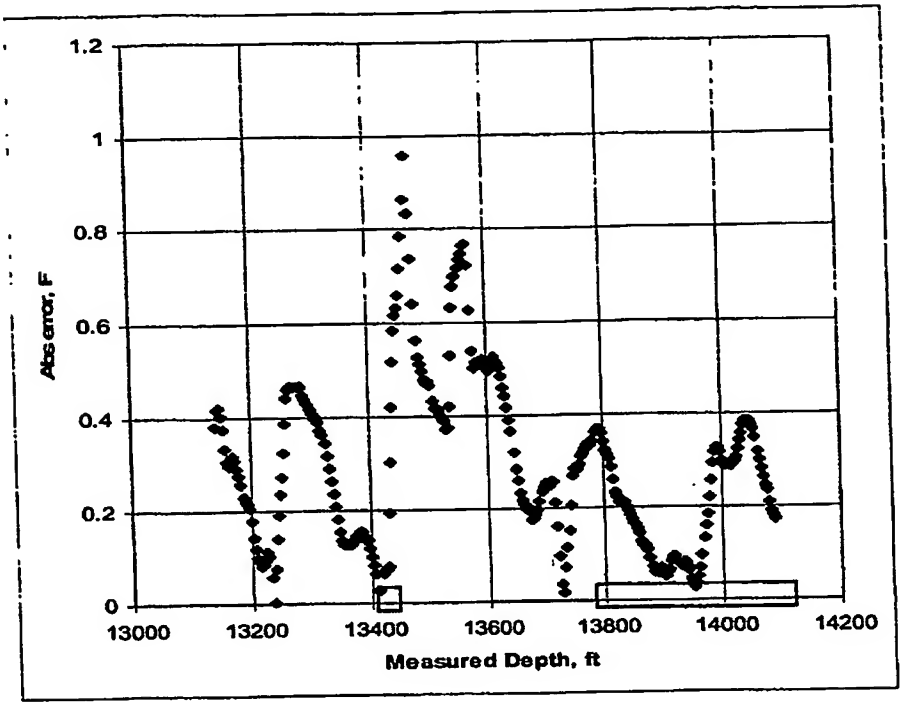

Fig. 5.4: Error comparison between the measured and the modeled

From Figs. 5.3 and 5.4, it should be noted that the modeled temperature is in good agreement with the measured temperature with a maximum difference less than 1 F. As seen from Fig. 5.4 that the higher error is in between the two producing zones, which might be due to the presence of the IC valve that complicates the physics of the problem and we did not take that into account in the modeling. Also for the inverse modeling, from tests that have been done before on each of two zones separately, it was noticed that the gross production from the lower zone is much higher than for the upper zone for both oil and water and that was captured from the inversion results. However, it is worth to mention that inversion was found to be highly depend upon the initial guess and that the problem is non unique problem and this finding support the results obtained from the synthetic examples where we showed for the two phase problem and small temperature contrast between the two zones it is very difficult to allocate the rate with high confidence due to the non uniqueness of the problem.

Chapter 6

CONCLUSIONS & RECOMMENDATIONS

[6.1] Conclusions

From this study, it can be concluded that:

1- A forward model of temperature has been developed from a basic theory of mass, momentum, and energy balance equations to describe the temperature profile in a single phase single layer producing well and tested against the numerical and the well known models in the literature and the results shows its good accuracy close to the producing intervals

2- The forward model has been extended to two zones two phase (oil-water) producing wells to be used as a forward tool in inverting for the zonal rate by knowing the temperature from DTS measurements

3- An inverse modeling using the GRG optimization algorithm coded in Excel is used to invert for the zonal rate allocation by minimizing the difference between the measured temperature from the DTS measurements and the calculated from the forward model

4- Several synthetic examples have been studied to test the validity and the accuracy of zonal rate allocation from DTS measurements in two layers producing wells under different conditions and the results reveal the following:

   i- For ***single-phase liquid*** production with ***high*** temperature contrast between the producing zones, the zonal rates can be allocated with good accuracy without imposing the total rate as constraint in the optimization problem

   ii- For ***single-phase liquid*** production with ***low*** temperature contrast between the producing zones, the zonal rates can be allocated with good accuracy if the total rate is added as constraint in the optimization problem.

   iii- ***For two-phase (oil-water)*** production with ***high*** temperature contrast between the producing zones, the zonal rates can be allocated with good

accuracy only after imposing the total rate for each production phase as constraint in the optimization problem.

iv- ***For two-phase (oil-water)*** production with ***low*** temperature contrast between the producing zones, the zonal rates are difficult to be allocated even if the total rate for each phase is added as constraint, the problem shows a high non-uniqueness and the optimization mainly depends on the starting guess of the rates. So, prior information to select a good starting guess for the rates, or another constraint can be added to the problem to make it well constraint and this might improve the accuracy of the inversion.

5- A simple Excel spreadsheet has been prepared to analyze a field DTS measurements from two zones two layers producing wells.

6- Both the forward and the inversion has been tested on a field data taken from Bugan-07 deviated well and the results show a good agreement of the forward model with the measured temperature from DTS within maximum difference of 1 F. Also the results of inversion show qualitatively a good agreement with the information about the zonal productivity.

[6.2] Recommendations

The following points are recommended for future work:

1- The Excel spreadsheet that was developed to handle the field case for two zone two phase producing wells can be extended for more than three zones and the extension is trivial. This allows for analyzing the DTS measurements from wells producing two phase (oil-water) or single phase (oil) from one, two or three zones in short time.

2- Extending the forward modeling for single-phase gas and multi phase flow (gas and liquid). The extension of the forward model for multi phase flow (gas and liquid) can definitely handle a single-phase gas production, thus the key is to extend the forward model to multi phase flow. The major difficulties in modeling a multi phase arising in finding a way to get the Joule Thomson coefficient and the pressure drop inside the well to substitute them in Eq. 2.26. Reference 7 has

mentioned a good way to get an approximate equation for the Joule Thomson coefficient for black oil models and also for the pressure drop. The pressure drop can be calculated from any multi phase pressure drop correlation while the Joule Thomson coefficient can be obtained as a rate weighting average between the liquid Joule Thomson coefficient obtained from Eq. 2.30 and that for gas which depends upon a first order derivative of the compressibility factor with respect to temperature, any correlation for the gas compressibility factor can be used to get this first order derivative.

REFERENCES

1- Al-Asimi, M., Butler, G., Brown, G., Hartog, A., Clancy, T., Cosad, C., Fitzgerald, J., Navarro, J., Gabb, A., Ingham, J., Kimminau, S., Smith, J., and Stephenson, K.: "Advances in Well and Reservoir Surveillance," Schlumberger Oilfield Review (winter 2002/2003) 14-35, vol. 14, No. 4.

2- Bird, R.B., Stewart, W.E., and Lightfoot, E.N.: "Transport Phenomena," John Wiley & Sons, New York, NY (2002).

3- Sagar, R., Doty, D.R., and Scmidt, Z.: "Predicting Temperature Profiles in a Flowing Well," SPEPE (Nov. 1991) 441-448.

4- McCain, W.D., Jr.: "The Properties of Petroleum Fluids," PennWell Books, Tulsa, Oklahoma (1990).

5- Dake, L.P.: "Fundamentals of Reservoir Engineering," Elsevier, Amsterdam, The Netherlands (2001)

6- Hasan, A.R., and Kabir, C.S.: "Heat Transfer During Two-Phase Flow in Well bores: Part I- Formation Temperature," paper SPE presented at the 66th Annual Technical Conference and Exhibition, Dallas, TX, Oct. 6-9, 1991

7- Alves, I.N., Alhanatl, F.J.S., and Shoham, O.: "A Unified Model for Predicting Flowing Temperature Distribution in Well bores and Pipelines," SPEPE (Nov. 1992) 363-367.

8- Beggs, H.D.: "Production Optimization Using Nodal Analysis," OGCI Publications, Tulsa, Oklahoma (1991).

9- Eclipse 100 and 300 Technical Description, Geoquest, 2001

10- Ramey, H.J. Jr.: "Well bore Heat Transmission," JPT (April 1962) 427-435; Trans., AIME, 225

11- Nocedal, J., and Wright, S.: "Numerical Optimization," Springer-Verlag, New York (1999)

12- Kincaid, D., and Cheney, W.: "Numerical Analysis: Mathematics of Scientific Computation," Brooks/Cole, Pacific Grove, CA (2002)

13- Lasdon, L.S.,Waren, A.D., Jain, A., and Ratner, M.: "Design and Testing of a Generalized Reduced Gradient Code for Non Linear Programming," ACM Transaction on Mathematical Software (March 1978), vol. 4, No. 1, 34-50.

14- Curtis, M.R., and Witterholt, E.J.: "Use of the temperature Log for Determining Flow Rates in Producing Wells," paper SPE 4637 presented at the 48th Annual fall meeting of the society of petroleum engineers of AIME, Las Vegas, Nevada, Sept. 30-Oct. 3, 1973

15- Popov, Yu., and Romushkevich, R.: "Thermal Conductivity of Sedimentary Rocks of Oil-Gas Fields," Schlumberger Internal Report